Electronic Supplementary Material (ESI) for Energy & Environmental Science.

Supporting information

for

Understanding the perovskite/self-assembled selective contact interface for ultra-stable and highly efficient p-i-n perovskite solar cells

Ece Aktas,[Ŧ,1,2] *Nga Phung,*[Ŧ,3,§] *Hans Köbler,*[3] *Dora A. González,*[1,4] *Maria Méndez,*[1] *Ivona Kafedjiska,*[5] *Silver-Hamill Turren-Cruz,*[3] *Robert Wenisch,*[5] *Iver Lauermann,*[5] *Antonio Abate*,*[3,6] *and Emilio Palomares*,*[1,7]

[1]Institute of Chemical Research of Catalonia (ICIQ-BIST). Avda. Països Catalans, 16. Tarragona. E-43007. Spain.

[2]Departament de Química-Física i Inorgànica. URV. E-43007. Spain.

[3]Helmholtz-Zentrum Berlin für Materialien und Energie GmbH, Kekuléstr. 5, Berlin D-12489, Germany.

[4]Departament d'Enginyeria Electrònica, Elèctrica i Automàtica. URV. Tarragona. E-43007. Spain.

[5]PVcomB/Helmholtz-Zentrum Berlin für Materialien und Energie GmbH, Schwarzschildstraße 3,12489 Berlin, Germany.

[6]Department of Chemical, Materials and Production Engineering, University of Naples Federico II, Piazzale Tecchio 80, 80125 Fuorigrotta, Italy.

[7]ICREA. Passeig LLuís Companys 23. E-08010. Spain.

[Ŧ]Contributed equally to this work.

[§]Present address: Department of Applied Physics, Eindhoven University of Technology, 5600 MB Eindhoven, the Netherlands.

Email of corresponding authors:

antonio.abate@helmholtz-berlin.de

antonio.abate@unina.it

epalomares@ICIQ.es

Table of Contents

1. Methods and Materials

1.1. *Syntheses of SAMs*

All reagents are purchased from Sigma-Aldrich, TCI Europe, Alfa Aesar and they are used as received without further purification unless otherwise stated. Common solvents are purchased from SdS. Toluene is distilled prior use. The synthesis of 3,6-bis(2,4-dimethoxyphenyl)-9*H*-carbazole is performed as our previously reported study.[1] 4-(3,6-bis(2,4-dimethoxyphenyl)-9*H*-carbazol-9-yl)benzoate (EADR03-COOEt) and 4'-(3,6-bis(2,4-dimethoxyphenyl)-9*H*-carbazol-9-yl)-[1,1'-biphenyl]-4-carboxylate (EADR04-COOMe) are synthesized through palladium-catalyzed Buchwald-Hartwig cross-coupling reaction using tris(dibenzylideneacetone)dipalladium(0) ($Pd_2(dba)_3$), tri-tert-butylphosphine tetrafluoroborate ((*tert*-Bu)$_3$P), sodium tert-butoxide (*tert*-BuO-Na$^+$).[2] The pure compound of EADR03 and EADR04 are hydrolyzed by potassium hydroxide in solvent mixture of methanol: tetrahydrofuran under reflux condition. The molecule structures of synthesized compound are confirmed by means of ^{1}H and ^{13}C Nuclear Magnetic Resonance Spectroscopy (NMR), High Resolution Mass Spectra (HR-MS) and Elemental Analysis. Structures of the synthesized compounds are confirmed by means of ^{1}H and ^{13}C NMR spectroscopy.

1.2. *Absorption measurements*

Absorption spectra are measured using 1 cm path length quartz cells in a Shimadzu UV spectrophotometer 1700 with optical range from 190 to 1100 nm at room temperature. All the measurements are carried out using toluene as solvent. The fluorescence spectra in solution are also recorded using 1 cm path length quartz cuvettes in Spectrofluorimeter Fruorolog from Horiba Jobin Yvon Lrd with a PMT(UV-vis) and InGaAs (NIR) detectors that allow fluorescence measurements in the wavelengths range from 250 to 1600 nm at room temperature. The energy of the optical bandgap is calculated accordingly to: $E_g = 1240/\ \lambda_{a.e.}$, where $\lambda_{a.e.}$ is the absorption edge wavelength onset and its value is taken from the intersection of the normalized absorption and emission spectra recorded in diluted solutions.

1.3. *Thermogravimetric analysis (TGA)*

TGA determines the rate and the weight loss of a phase as a function of temperature or time under a controlled atmosphere. The measurements are carried out in a TGA/SDTA851 Mettler Toledo equipment. The working temperature went from 30 °C to 600 °C at a scan rate of 10 °C/min under nitrogen atmosphere. The decomposition temperature is considered when the samples loss up to 5 % of its initial weight.

1.4. *Differential Scanning Calorimetry (DSC)*

DSC analysis provides information about physical and chemical changes that involve endothermic and exothermic processes, or changes in the heat capacity. DSC analysis are measured in DSC822e Mettler Toledo calorimeter. The working temperatures went from 30 °C to 450 °C performing three continuous cycles, at a scan rate of 10 °C/min. The glass transition temperatures for the investigated compounds are determined during the second and third heating scan under nitrogen atmosphere.

1.5. ^1H and ^{13}C Nuclear Magnetic Resonance Spectroscopy (NMR)

^1H and ^{13}C NMR spectra are recorded on a Bruker Avance 400 (400 MHz for ^1H and 100 MHz for ^{13}C). The deuterated solvents used are indicated; chemical shifts, δ, are given in ppm, referenced to the solvent residual signal (^1H, ^{13}C). Coupling constants, *J*, are given in Hz.

1.6. High Resolution Mass Spectra (HR-MS)

High Resolution Mass Spectra (HR-MS) are recorded on a Waters LCT Premier liquid chromatograph couple time-of-flight mass spectrometer (HPLC/MS-TOF), using electro spray ionization (ESI) as ionization mode.

1.7. Device Fabrication

The patterned indium tin oxide (ITO) glass substrates (25x25 mm, 15 Ω sq-1, commercialized available at Automatic Research GmbH), are cleaned for 15 minutes with Mucasol 2% solution in deionized water, Acetone, and Isopropanol in an ultrasonic bath. The layers are then dried well before treated in an UV-ozone cleaner for 15 min. After UV-ozone treatment, the ITO substrates immediately are transferred to N_2 filled glovebox.

EADR03 powder is easily soluble in non-halogenated organic solvent for using dipping and spin coating deposition methods at 60 ˚C. EADR04 solution temperature is raised up to 60 ˚C for increasing solubility in non-halogenated organic solvents before dipping. EADR04 did not show good results with spin-coating method. The molarity of EADR03 are approximately 0.1 mM and 1 mM in solvents for spin coating and dipping method, respectively. For spin coating method, 100 µL of the SAM solution are homogeneously poured onto the treated ITO and deposited by spin-coating at 3000 rpm for 30 seconds.

For dipping method, the treated ITO substrates are fully submerged in the solutions. After 4 hours of dipping, the SAM-HSL films onto ITO substrates are dried from excess solution. Afterwards, 500 µL of fresh anhydrous solvent which is the one used for preparing SAM solution are poured onto SAM-HSL covered ITO. Washing step is necessary and easy way for removing non-bonded SAM molecules from metal oxide surface by spin-coating at 3000 rpm for 30 seconds.

To make PTAA layers, PTAA (Sigma Aldrich) is dissolved at a concentration of 2 mg/mL in dry Toluene (Sigma Aldrich). The deposition is performed by spin-coating at 5000 rpm for 30 seconds and annealing at 100°C for 10 minutes in glove box.

The CsFAMA perovskite solution detailed preparation is reported elsewhere[3]. Briefly, $PbBr_2$ (1.5M) and PbI_2 (1.5M) are dissolved in a mixture of anhydrous Dimethylformamide (DMF): Dimethyl sulfoxide (DMSO) (4:1 volume ratio) (Sigma Aldrich) and added to formamidinium iodide (FAI, Dyenamo, 99.99%) (1.09:1 molar ratio) and methylammonium bromide (MABr, Dyenamo, 99.99%) (1.09:1 molar ratio) powders respectively, to obtain $MAPbBr_3$ and $FAPbI_3$ solutions with a final concentration of 1.24 M. These two solutions are then mixed in a 17:83 volume ratio.

Finally, the cesium cation is added from a 1.5 M CsI (abcr gmbh, 99%) solution in DMSO in a 5:95 volume ratio. The perovskite solution is spin-coated on top of the HTM layer using the following program: 4000 rpm (5 s acceleration) for 35 s (program's total time is 40 s). After 25 s, 250 µl of Anisole (Sigma Aldrich) is dropped on the spinning substrate to promote fast solvent-removal forming a smooth and compact layer. After the spin-coating program, the perovskite-coated sample is annealed at 100°C for 60 min. In the case where LiF is used, 1 nm LiF is evaporated on top of perovskite. Subsequently, 23 nm of C_{60} and 9 nm of bathocuproine (BCP) are evaporated on top of perovskite with rate of 0.5-0.2 Å/s. 100 nm NaF is evaporated on the glass side after complete full device as antireflection coating. Finally, 100 nm of Cu (Alfa Aesar, 99.99%) is evaporated with rate less than 1 Å/s as the metal electrode.

In the case where SnO_2 is replaced BCP, the perovskite layers are annealed only for 30 minutes instead of full one hour. The SnO_2 is fabricated using atomic layer deposition (ALD). The precursor used in this study is TDMASn (Tetrakis(dimethylamido)tin(IV)) and co-reactant is water. The precursor temperature is 60 °C, and the table temperature is 80 °C. The precursor/water dosing steps are 1s and 0.2s respectively. After each precursor dosing step, there is one purging step for 10s, and similarly after water dose, the chamber is purged for 15s.

1.8. Current Density-Voltage Scan

Current-voltage (J-V) characteristics under 1 sun equivalent illumination using Oriel LCS-100 class ABB solar simulator in an inert atmosphere for the J-V measurement. The sun simulator is calibrated with a Fraunhofer ISE silicon diode to assure a light intensity of 100 mW/cm^2. The scan rate is 100 mV/s starting from forward scan (V_{OC} to J_{SC}) using Keithley Model 2400 as a voltage source.

1.9. External Quantum Efficiency Measurement (EQE)

EQE measurements are recorded by an Oriel Instruments QEPVSI-b system with a Xenon lamp (Newport 300 W). The white light is chopped at a frequency of 78 Hz by a Newport Cornerstone 260 monochromator. Before each measurement, a Si diode with a known spectrum is used as reference. The response from the solar cells is measured with a Stanford Research SR830 Lock-In amplifier and evaluated by a commercial software named TracQ.

1.10. Scanning Electron Microscope (SEM)

The SEM images are acquired with Hitachi S4100 at 30k magnification. The voltages used for SEM is 5 keV.

1.11. X-ray Diffraction (XRD)

XRD measurements are conducted in the air with the PANalytical X'Pert Pro MPD (multi-purpose diffractometer) using grazing incidence geometry. Grazing incident X-ray diffraction (GIXRD) patterns are collected with a step size of 0.02 degree, for 6 seconds each step. For this measurement, a 20 nm of PMMA layer (20 mg/mL in chlorobenzene, Sigma Aldrich) was spin-coated on perovskite to protect the layer in air.

1.12. X-ray Photoelectron Spectroscopy (XPS) and Ultra-violet Photoelectron (UPS)

In order to study the chemical state of the atoms of the compounds XPS measurements are performed using Mg Kα radiation (hv = 1253.6 eV, P = 150 W) to excite the photoelectrons with a XR50 (SPECS) X-ray source. It houses a CLAM 4 (VG) electron analyzer for photoemission (PES) spectroscopy. The measurements are carried out in the CISSY ultra-high vacuum apparatus (base pressure: $p < 2\times10\text{-}8$ mbar). The X-ray source and the analyser are arranged under a fixed 54° "magic" angle. More details on the setup are available elsewhere.[4]

Using the same machine, UPS measurements were done, employing He I radiation ($hv = 21.22$ eV) from a He discharge lamp yielding the energy offset of the HOMO from the Fermi level. For the UPS measurements the samples were biased with -15 V vs. ground to facilitate the emission of the secondary electrons.

The XPS spectra were corrected for charging by referencing the 4f transition of a gold reference to 84.0 eV. The spectra were then analysed by subtracting a Shirley-type background approximation and fitting Voigt-type peaks[5] to the remaining signal. The Lorentzian FWHM was constrained to 0.6 eV while the Gaussian FWHM was allowed to float within a range of 0.7-1.2 eV. The peak centres were constrained to value ranges to prevent overlapping or peaks exchanging positions, but care was taken not to allow values to run into the constraining limits. Peak areas were constrained to only to assume values ≥ 0.

1.13. Contact Angle Measurement

Contact angle measurements are carried out with a Kruss Drop Shape Analysis System DSA25.

1.14. Steady-State Fluorescence Emission

Steady state fluorescence emission measurements are performed on a Fluorolog Horiba Jobin Yvon spectrofluorometer equipped with photomultiplier detector, double monochromator and Xenon light source.

1.15. Time-Correlated Single Photon Counting Measurements (TCSPC)

Lifetime measurements are performed on an Edinburgh Instruments LifeSpec-II based on the TCSPC technique, equipped with a PMT detector, double subtractive monochromator and 470 nm picosecond pulsed diode lasers source. All perovskite films are protected with PMMA to do measurements in the ambient condition.

1.16. Maximum Power Point (MPP) Tracking of Perovskite Solar Cells

A custom-built High-throughput Ageing Setup is used for the ageing test of perovskite solar cells.[6] Each cell is individually MPP-tracked by the use of special electronics. A perturb and observe[7] algorithm with a voltage step-width of 0.01 V and a delay time of 1s is applied to track the MPP. PCE_{MPP} tracking values are automatically recorded for all cells every 2 minutes and normalised to the start value. During the tracking, the active area is touching a heat pad in order to ensure direct thermal coupling and Peltier-elements are used for cooling and keep the cells at 25 °C at all time. MPP tracking of devices is performed without encapsulation and under a continuous flow of nitrogen in a closed box. A metal-halide lamp with H2 filter is used as a light source with 100 mW/cm^2 intensity. A comparison of the spectrum of the light source with H2 filter to AM1.5G are shown in Figure S21a. The light source intensity is actively controlled using a silicon irradiation-sensor which itself is calibrated using a Silicon reference from Fraunhofer ISE. For experiments with UV-filter, the UV-blocking foil “KFU15” by Mitsui is used to block UV light with wavelengths below 380 nm. The transmittance of the UV-blocking foil (in text named UV filter) is shown in Figure S21b. The light source intensity reaching the solar cells tested with UV-filter is measured to be approximately 80 mW/cm^2 due to the filter and its diffusing properties. The ageing test is in accordance with the ISOS-L-1I protocol. The UV-induced degradation is carried out with a Vilber Lourmat VL-6.L lamp. The power of the UV tube is 6 Watt. All HSLs deposited ITO substrates have been exposed to 365 nm for 30 minutes before perovskite deposition.

2. Thermogravimetry Measurements and Differential Scanning Calorimetry Measurements

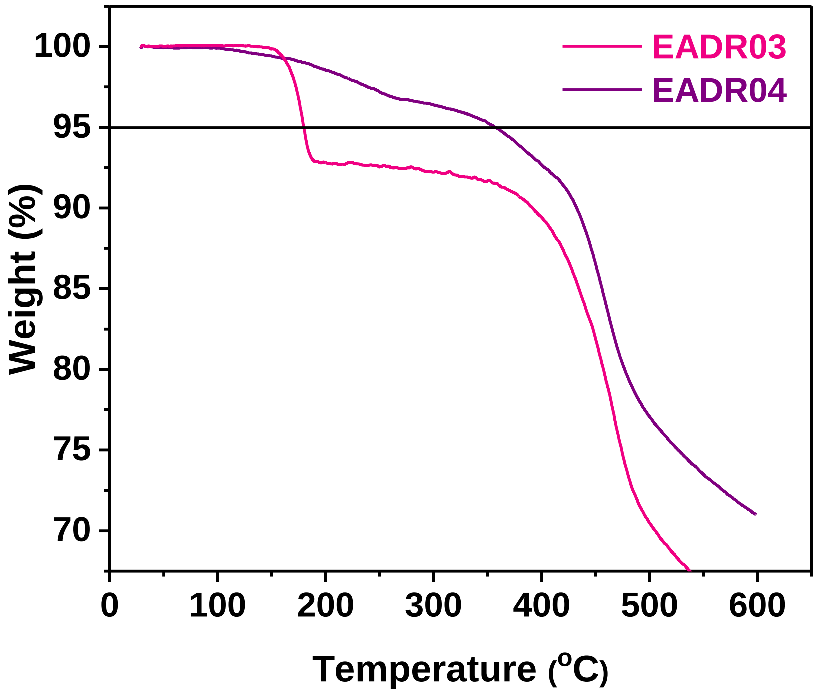

Figure S1. *TGA analysis of EADR03 and EADR04.*

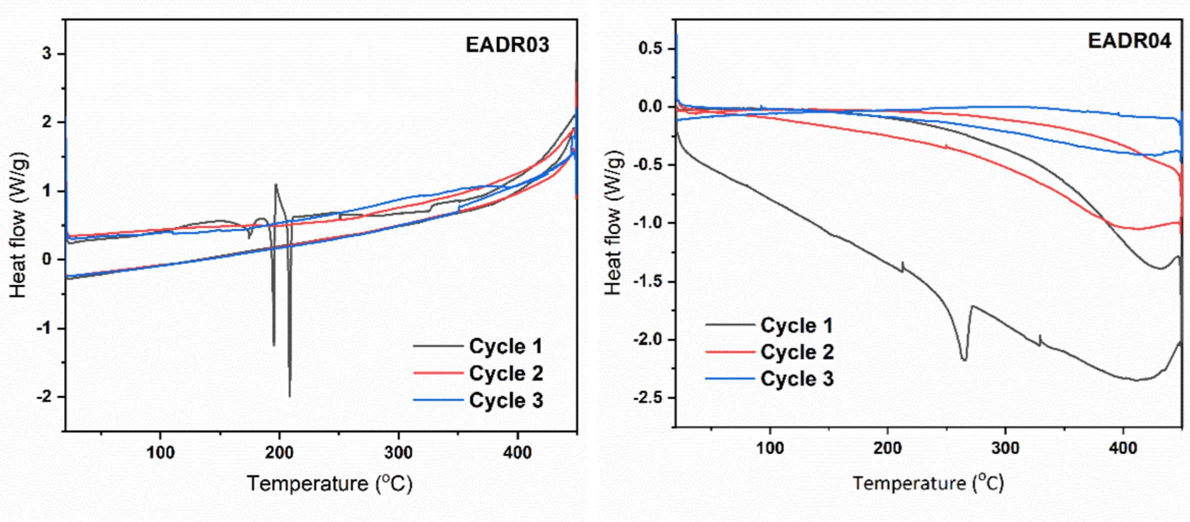

Figure S2. *DSC analysis of EADR03 and EADR04.*

Table S1. *Thermal properties of EADR03 and EADR04.*

HTMs	*T_{des} (°C)* [a]	*T_g (°C)* [b]
EADR03	180	173
EADR04	354	354

[a] Decomposition temperature determined from TGA (5 % weight loss). [b] Glass transition temperature determined from the second cycle of DSC. All experiments were carried out under N_2 atmosphere, scan rate of 10 °C/min.

3. Optical Measurements of EADR03 and EADR04

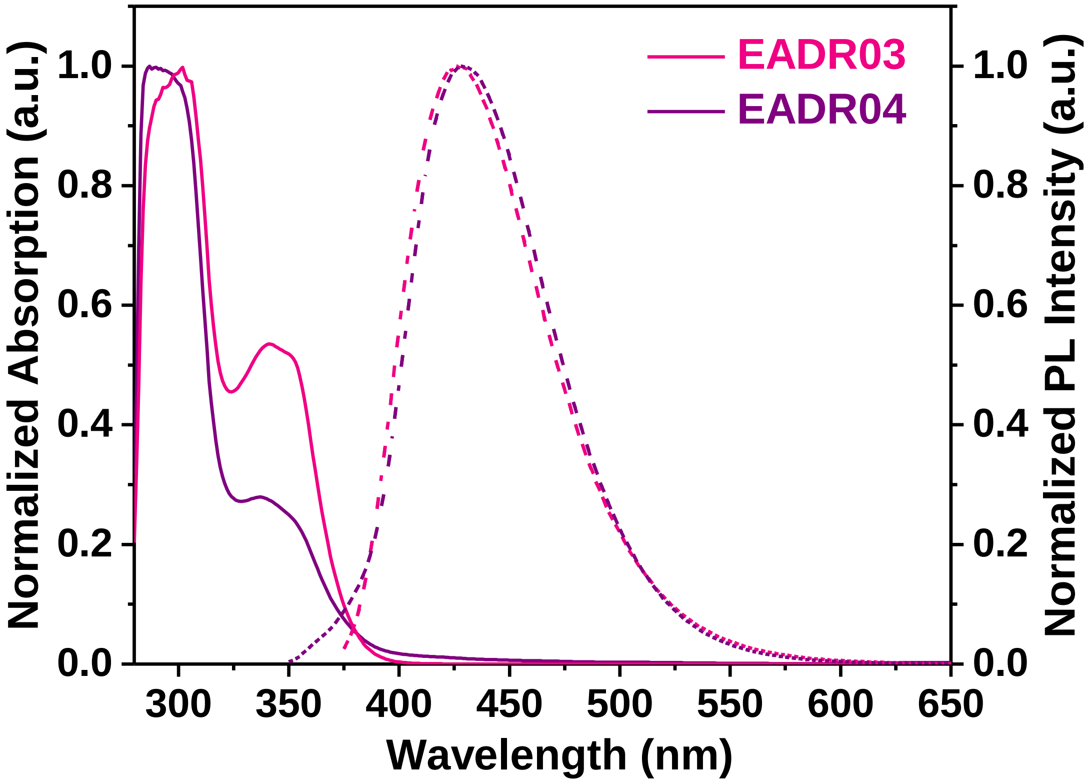

Figure S3. *Absorption (solid lines) and emission (dashed lines) spectra of EADR03 and EADR04.*

Table S2. *Optical and energetic properties of small molecules.*

SAMs	*$\lambda_{abs.}$ (nm)*	*$\lambda_{em.}$ (nm)*	*$\lambda_{a.e.}$ (nm)*	*$E_g^{opt.}$ (eV)*	*LUMO (eV)*
EADR03	300/345	425	378	3.28	**1.77**
EADR04	290/335	430	374	3.31	**1.74**

4. SAM layers characterisation

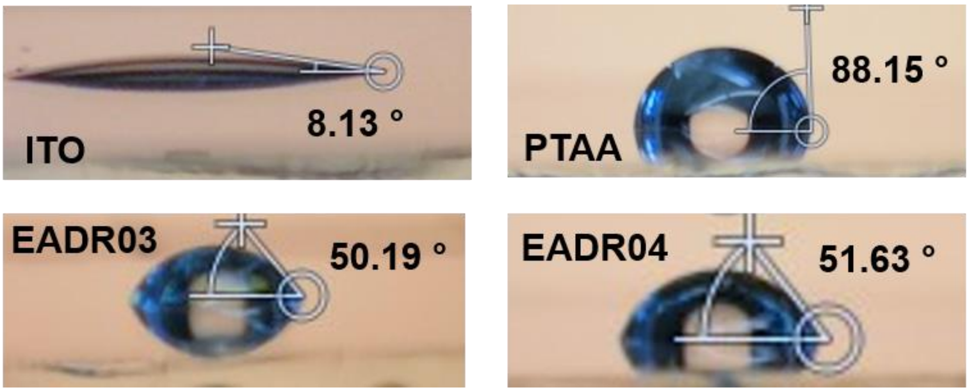

Figure S4. *Contact angle measurements on the bare ITO, ITO/PTAA ITO/EADR03, and ITO/EADR04 surfaces.*

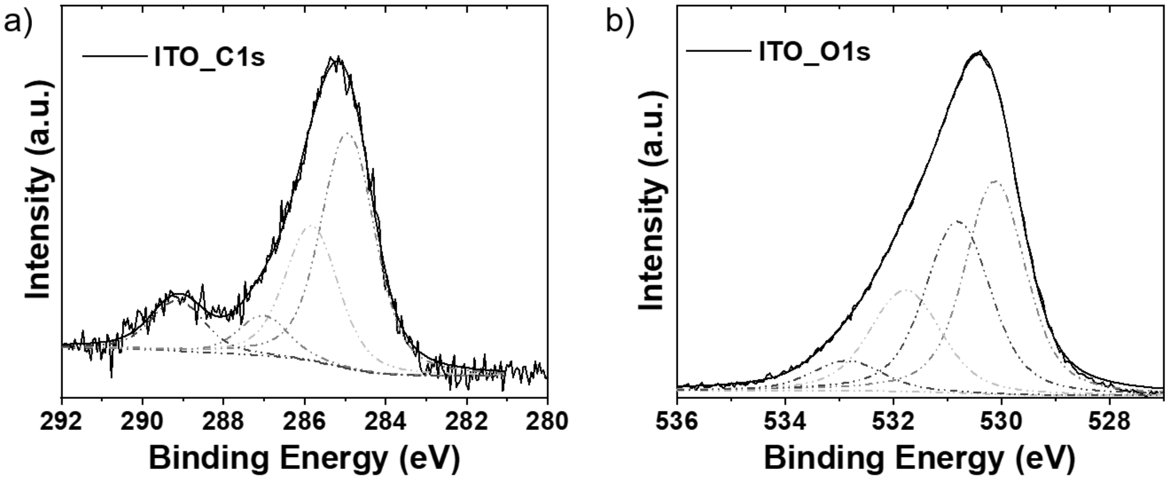

Figure S5. *The XPS high-resolution survey spectra of a) C1s and b) O1s for UV-Ozone treated ITO*

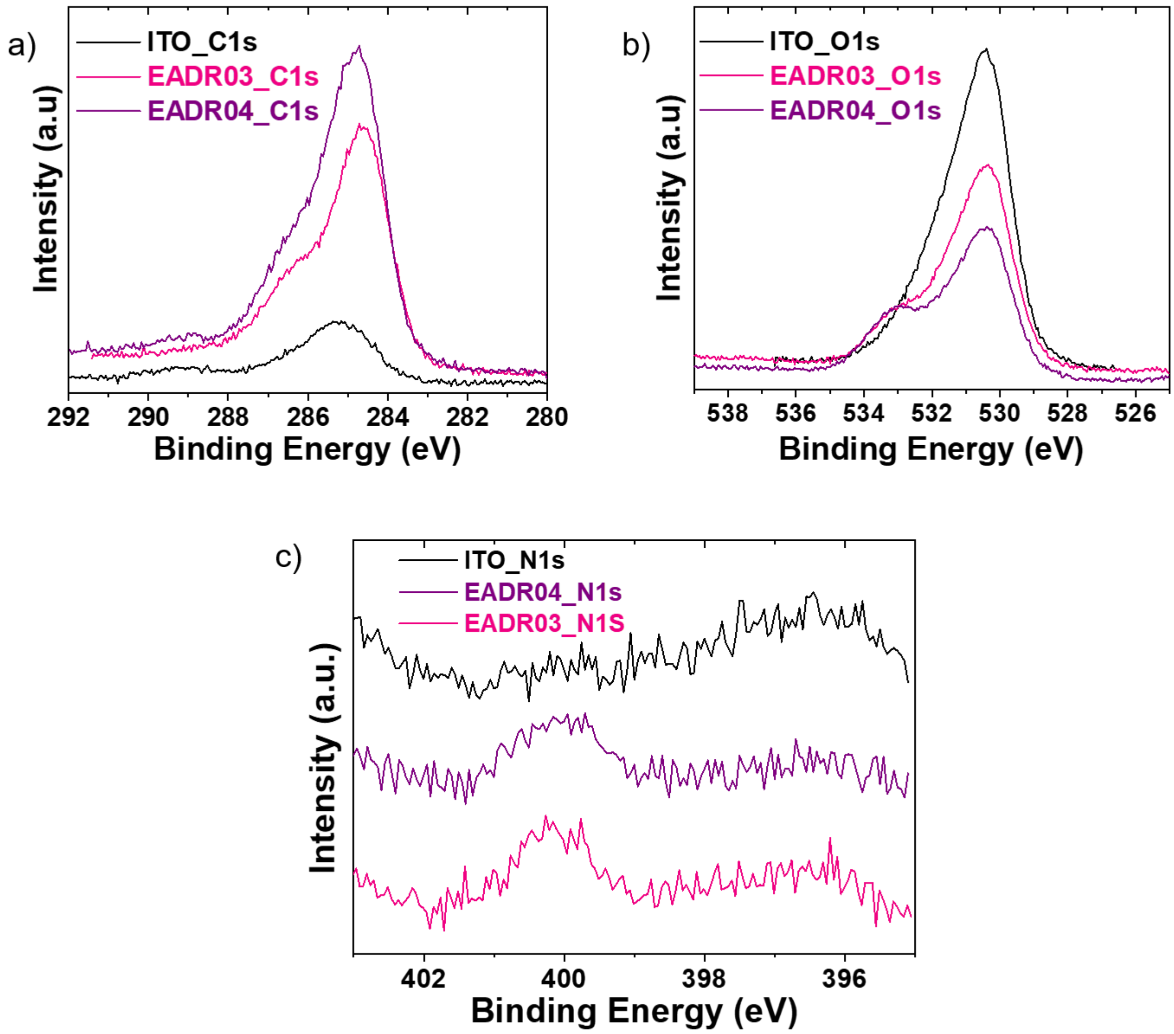

Figure S6. *The X-ray photoelectron spectroscopy at the a) C1s and b) O1s c) N1s regions of ITO glass with and without SAMs. The bare ITO has residual signals in these regions due to transferring samples between glovebox.*

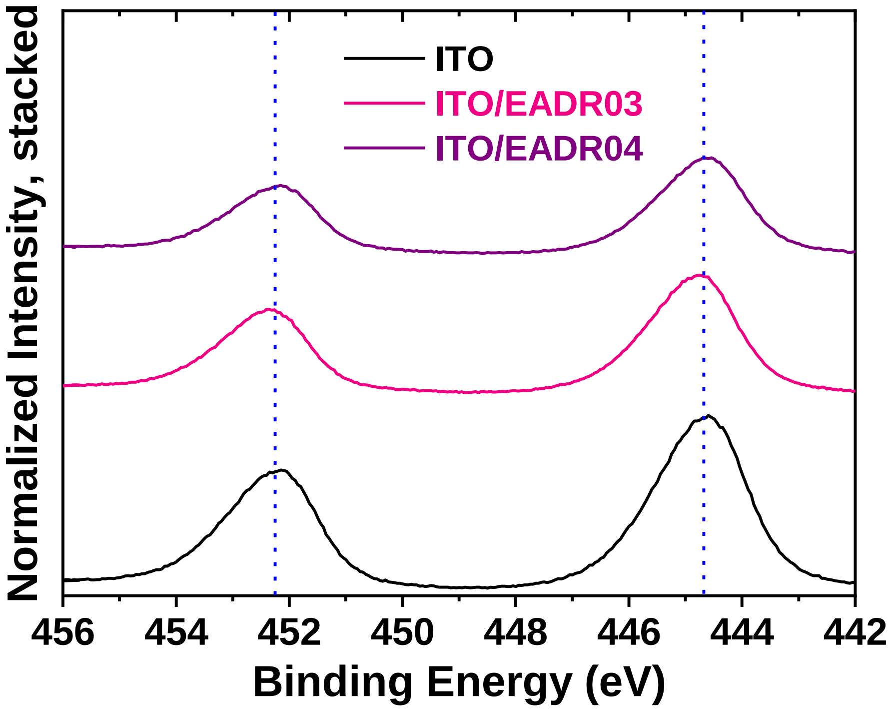

Figure S7. *The In peaks of the ITO substrates with and without SAM, which are measured using XPS after finishing the UPS measurement.*

Table S3. *Fit results for the C1s and O1s regions*

ITO C1s

Peak	***BE (eV)***	***Intensity (a.u.)***	***Gaussian FWHM (eV)***	***Lorentzian FWHM (eV)***	***Total FWHM (eV)***
C-C/C-H	284.9	2959	0.6	1.20	1.55
C-O	285.8	1701	0.6	1.20	1.55
O-C=O att.	287.0	482	0.6	1.20	1.48
O-C=O	289.1	635	0.6	1.20	1.55

ITO O1s

Peak	***BE (eV)***	***intensity (a.u.)***	***Gaussian FWHM (eV)***	***Lorentzian FWHM (eV)***	***Total FWHM (eV)***
ITO	530.1	34747	0.6	0.95	1.31
hydroxides	530.8	29983	0.6	1.07	1.43
C=O	531.8	18990	0.6	1.20	1.55
C-O	532.9	5591	0.6	1.20	1.55

EADR03 C1s

Peak	***BE (eV)***	***Intensity (a.u.)***	***Gaussian FWHM (eV)***	***Lorentzian FWHM (eV)***	***Total FWHM (eV)***
C-C/C-H	284.6	14194	0.6	1.10	1.45
C-O	286.0	4712	0.6	1.20	1.55
O-C=O att.	287.0	1438	0.6	0.94	1.30
O-C=O	288.5	120	0.6	0.80	1.17

EADR03 O1s

Peak	***BE (eV)***	***Intensity (a.u.)***	***Gaussian FWHM (eV)***	***Lorentzian FWHM (eV)***	***Total FWHM (eV)***
ITO	530.1	25875	0.6	1.04	1.40
hydroxides	530.9	18607	0.6	1.20	1.55
C=O	531.8	8765	0.6	1.20	1.55
C-O	533.1	7968	0.6	1.16	1.51

EADR04 C1s

Peak	***BE (eV)***	***Intensity (a.u.)***	***Gaussian FWHM (eV)***	***Lorentzian FWHM (eV)***	***Total FWHM (eV)***
C-C/C-H	284.7	17351	0.6	1.05	1.41
C-O	285.9	7293	0.6	1.20	1.55

O-C=O att.	287.0	2340	0.6	0.87	1.24
O-C=O	289.2	636	0.6	1.08	1.44

EADR04 O1s

Peak	***BE (eV)***	***Intensity (a.u.)***	***Gaussian FWHM (eV)***	***Lorentzian FWHM (eV)***	***Total FWHM (eV)***
ITO	530.1	15265	0.6	0.96	1.32
hydroxides	530.8	17432	0.6	1.20	1.55
C=O	531.9	7454	0.6	1.20	1.55
C-O	533.2	10129	0.6	1.20	1.55

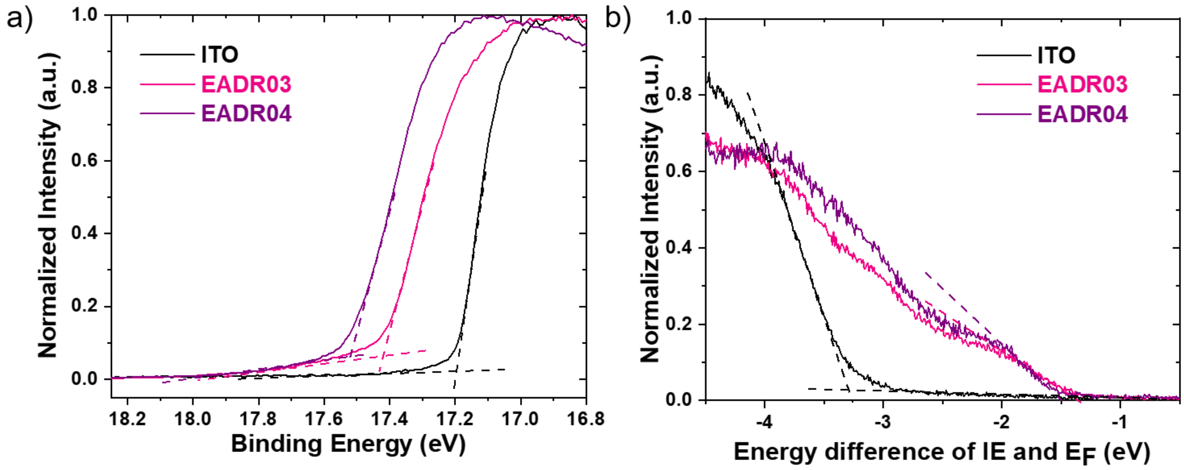

Figure S8. *Ultra-violet photoelectron spectra (UPS) of the SAMs on ITO a) the work function and b) valence band onset values are extracted for the energy band edge diagram in Fig. 1b of the main text (the excitation energy is 21.22 eV).*

5. Perovskite Layers Characterization

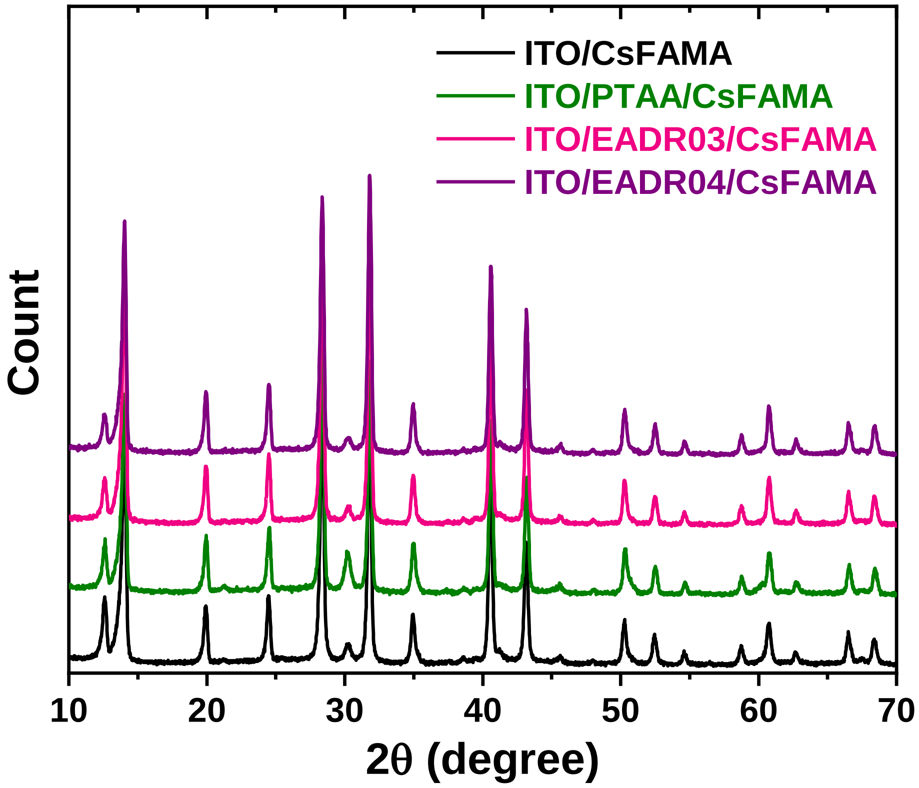

Figure S9. *X-ray diffraction patterns of perovskite layers grown on bare ITO, ITO/PTAA, ITO/EADR03 and ITO/ EADR04. The patterns are well in agreement with literature containing similar perovskite compounds.*[8,9]

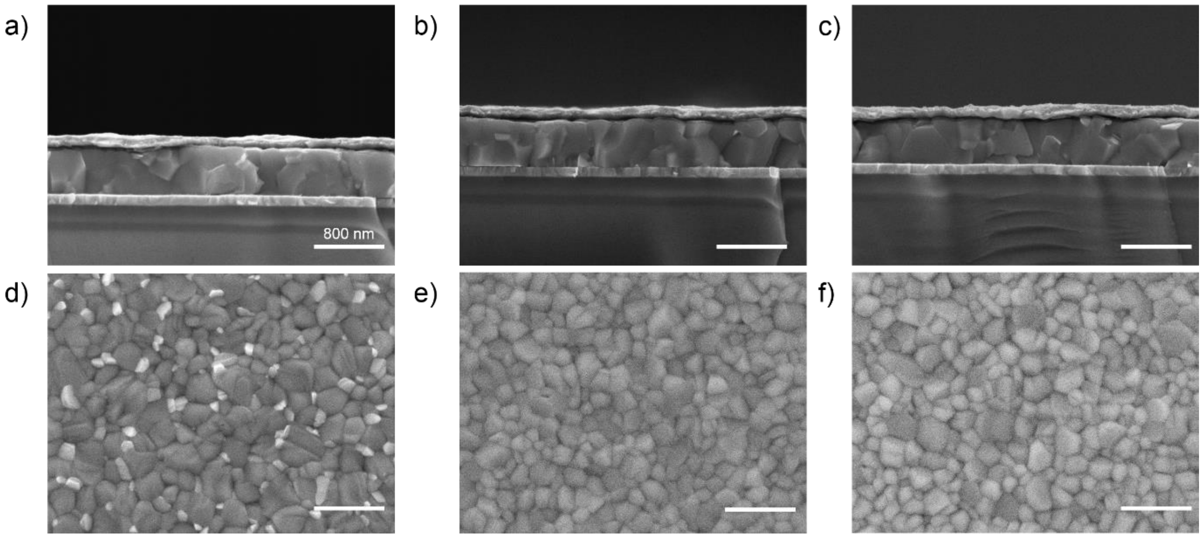

Figure S10. *Scanning electron microscopic images of cross-sectional full device of a)PTAA, b)EADR03 and c) EADR04 employed planar PiN perovskite solar cells; and top view of perovskite layers grown on d)ITO/PTAA, e)ITO/EADR03 and f) ITO/EADR04. All scale bars are 800 nm.*

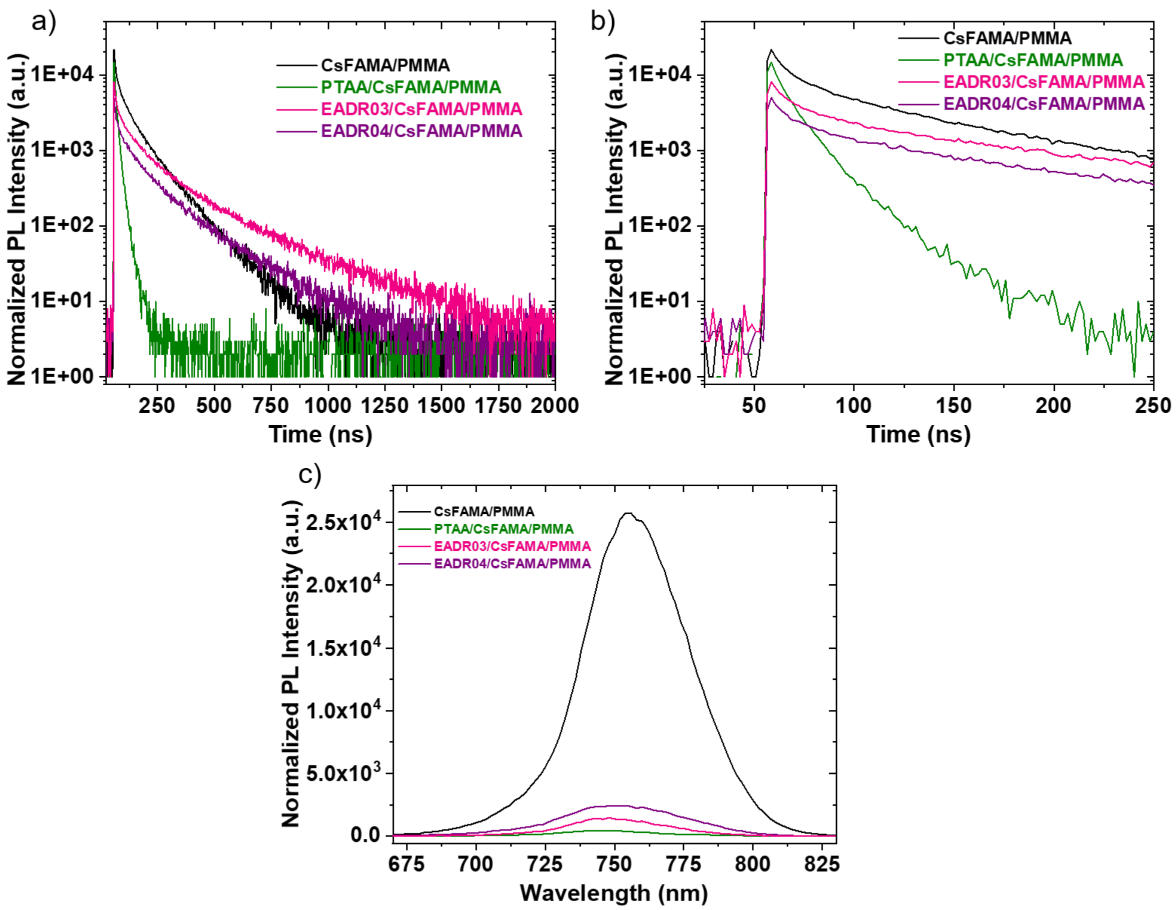

***Figure S11**. Luminescence emission decays (λ_{ex}=470 nm) measured for a) 2000 ns and b) 250 ns for CsFAMA/PMMA, the PTAA/CsFAMA/PMMA, EADR03/CsFAMA and EADR04/CsFAMA/PMMA on ITO coated glass substrate at room temperature. c)Luminescence emission band upon excitation at λ_{ex}=470 nm for the CsFAMA/PMMA, the PTAA/CsFAMA/PMMA, EADR03/CsFAMA and EADR04/CsFAMA/PMMA (total thickness of 550-600 nm) at room temperature.*

***Table S4.** Fitting values are obtained from the de-convolution of the luminescence decays in Figure S6b.*

Films	**τ_1 (ns)**	**τ_2 (ns)**
CsFAMA/PMMA	7	83
PTAA/CsFAMA/PMMA	2	12
EADR03/CsFAMA/PMMA	15	158
EADR04/CsFAMA/PMMA	9	106

6. Device statistic

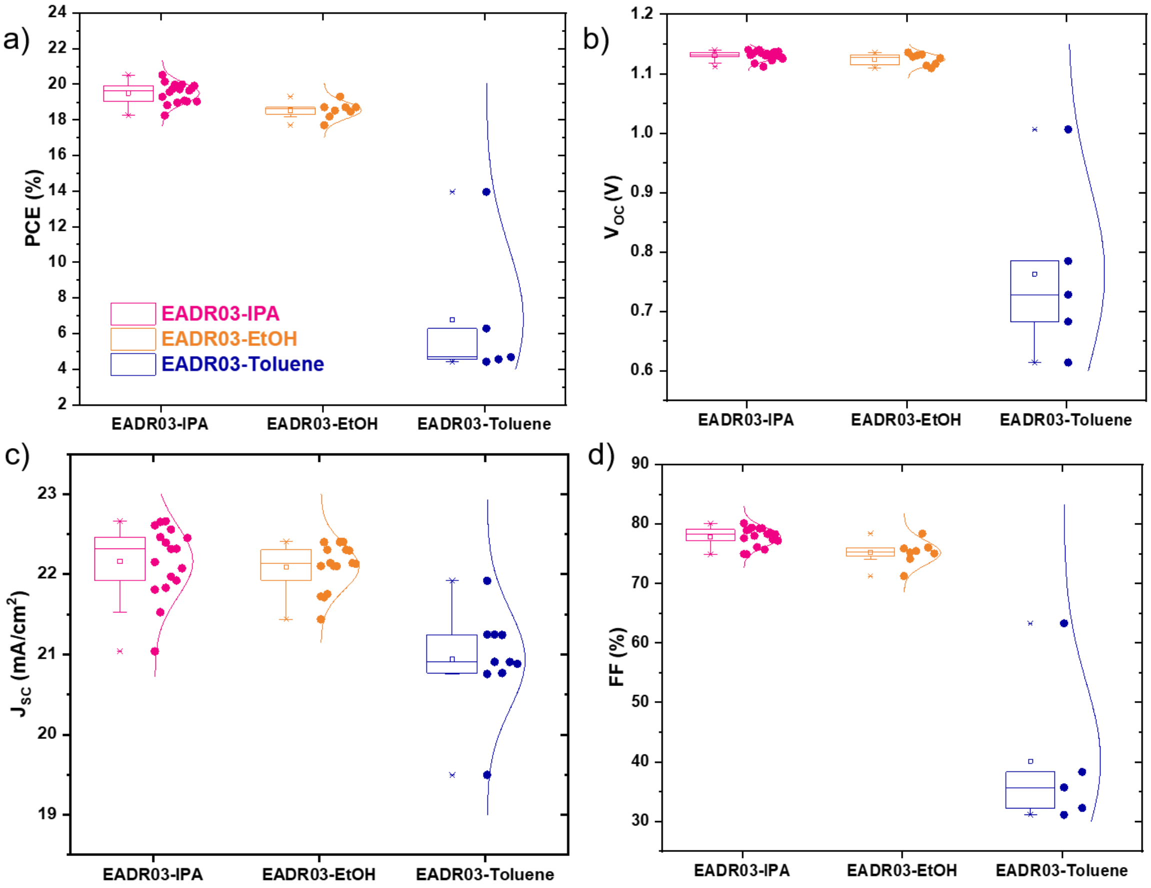

Figure S12. *Device performance statistic total 30 devices from EADR03 in different solvents in the devices a) PCE, b) V_{OC}, c) J_{SC}, d) FF.*

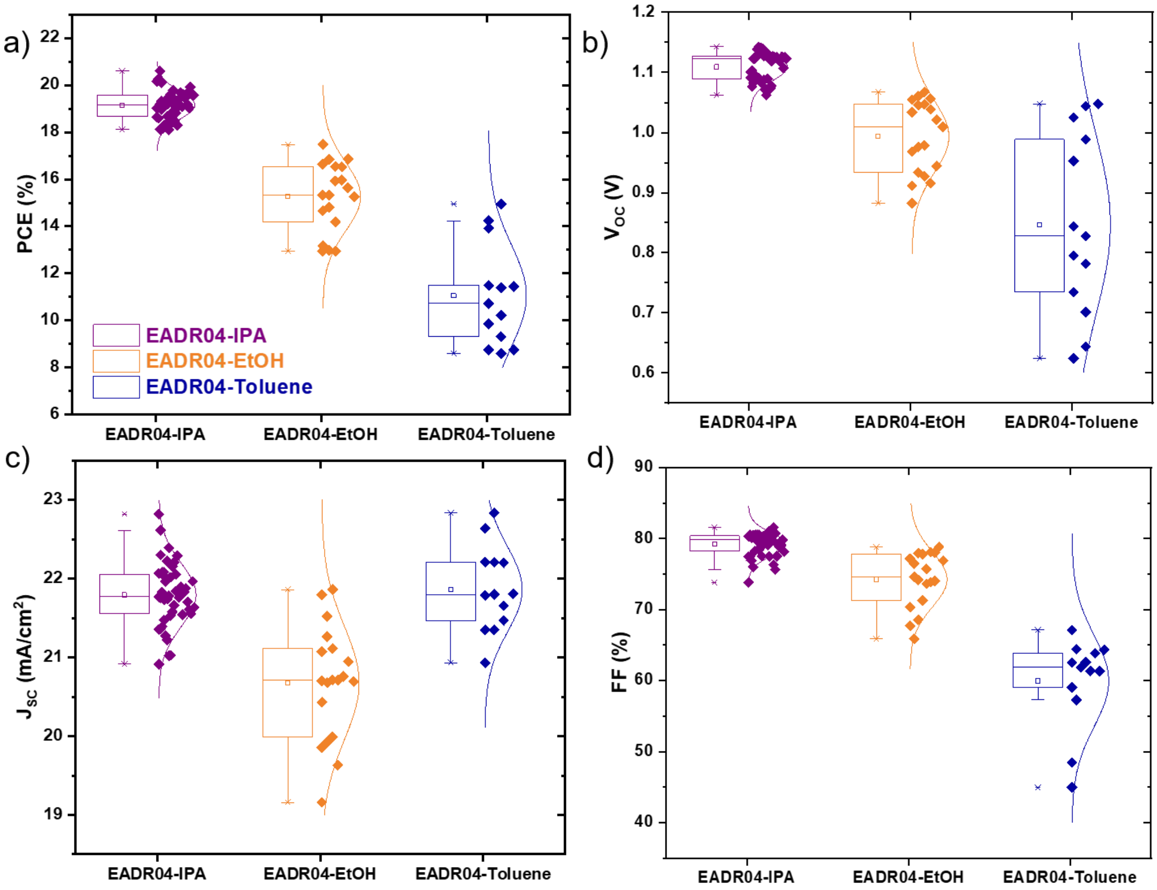

Figure S13. *Device performance statistic over 10 devices per conditions from EADR04 in different solvents in the devices a) PCE, b) V_{OC}, c) J_{SC}, d) FF.*

Table S5*. Best photovoltaic parameters from EADR03 and EADR04 in different solvents.*

SAMs	***Solvents***	***Scan Direction***	***Jsc (mA/cm^2)***	***V_{OC} (mV)***	***FF (%)***	***PCE (%)***
EADR03	IPA	fwd	22.6	1127	80	20.4
		rev	22.6	1132	80	20.5
EADR03	EtOH	fwd	21.7	1130	79	19.4
		rev	21.7	1132	78	19.2
EADR03	Toluene	fwd	21.9	993	61	13.3
		rev	21.9	1006	63	13.9
EADR04	IPA	fwd	22.6	1140	80	20.6
		rev	22.6	1143	79	20.4
EADR04	EtOH	fwd	20.7	1038	74	15.9
		rev	21.1	1083	77	17.6
EADR04	Toluene	fwd	22.2	1025	62	14.1
		rev	22.2	1037	62	14.3

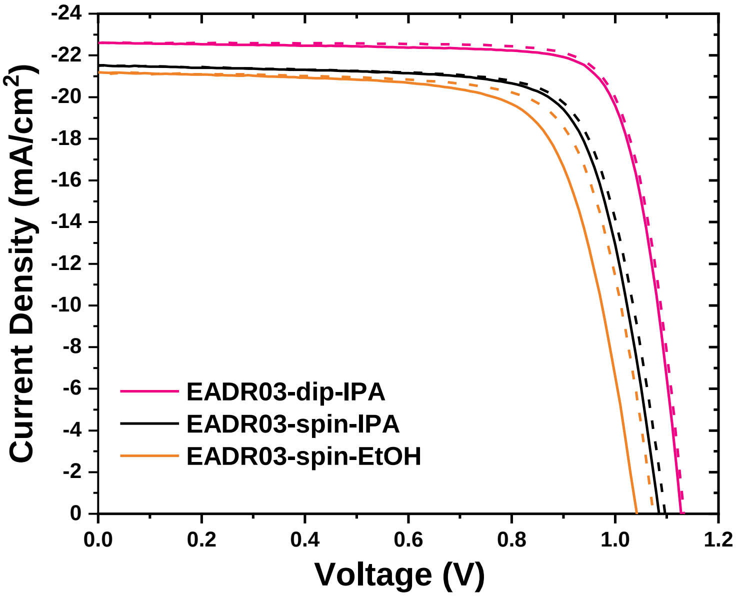

Figure S14. *Best J-V curves from EADR03 with different deposition methods.*

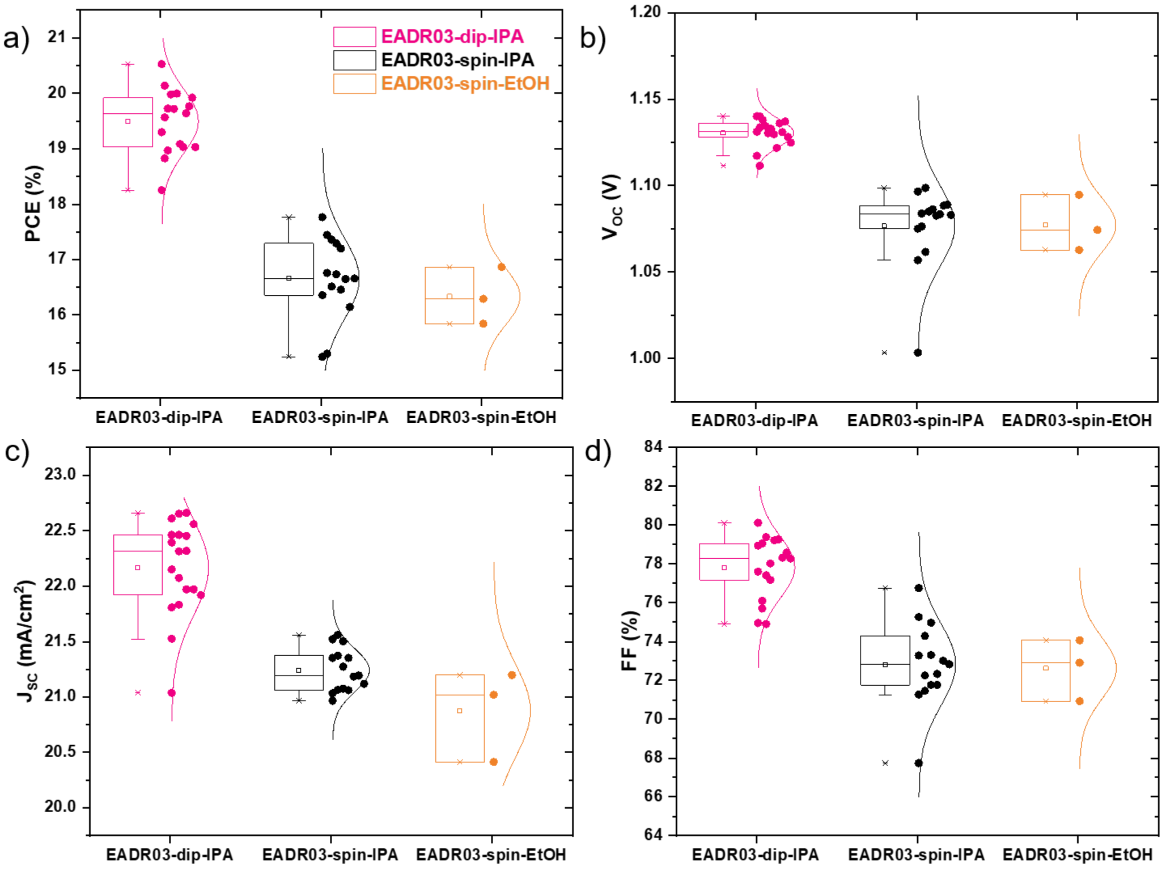

Figure S15. *Device performance statistic total 30 devices using different deposition methods of EADR03 in the devices a) PCE, b) V_{OC}, c) J_{SC}, d) FF. Forward and reverse scan value plotting together.*

Note: Spin coating doesn't work with EADR04 (no statistic)

Table S6. *Photovoltaic parameters from EADR03 with different deposition methods.*

SAMs	***Deposition Method***	***Solvents***	***Scan Direction***	***Jsc (mA/cm^2)***	***V_{OC} (mV)***	***FF (%)***	***PCE (%)***
EADR03	Dipping	IPA	fwd	22.6	1127	80	20.4
			rev	22.6	1132	80	20.5
EADR03	Spin Coating	IPA	fwd	21.5	1084	75	17.5
			rev	21.5	1096	75	17.7
EADR03	Spin Coating	EtOH	fwd	21.2	1041	72	15.9
			rev	21.2	1074	74	16.9

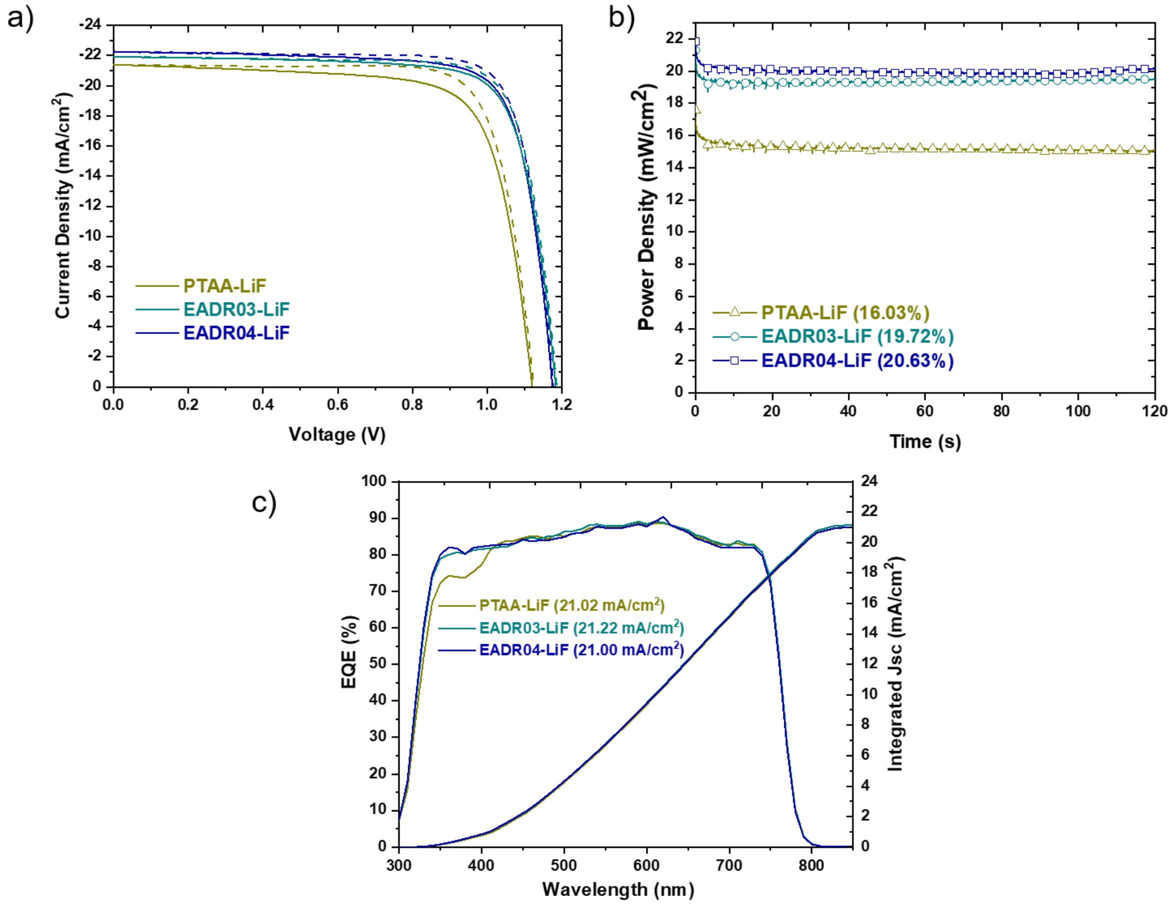

Figure S16*. a) Best J-V curves from PTAA, EADR03 and EADR04 with LiF. b) Quasi-steady state efficiency of charge selective contacts with LiF employed perovskite solar cells. c) Corresponding external quantum efficiency curves which shows integrated current density in agreement with values from J-V measurement with LiF.*

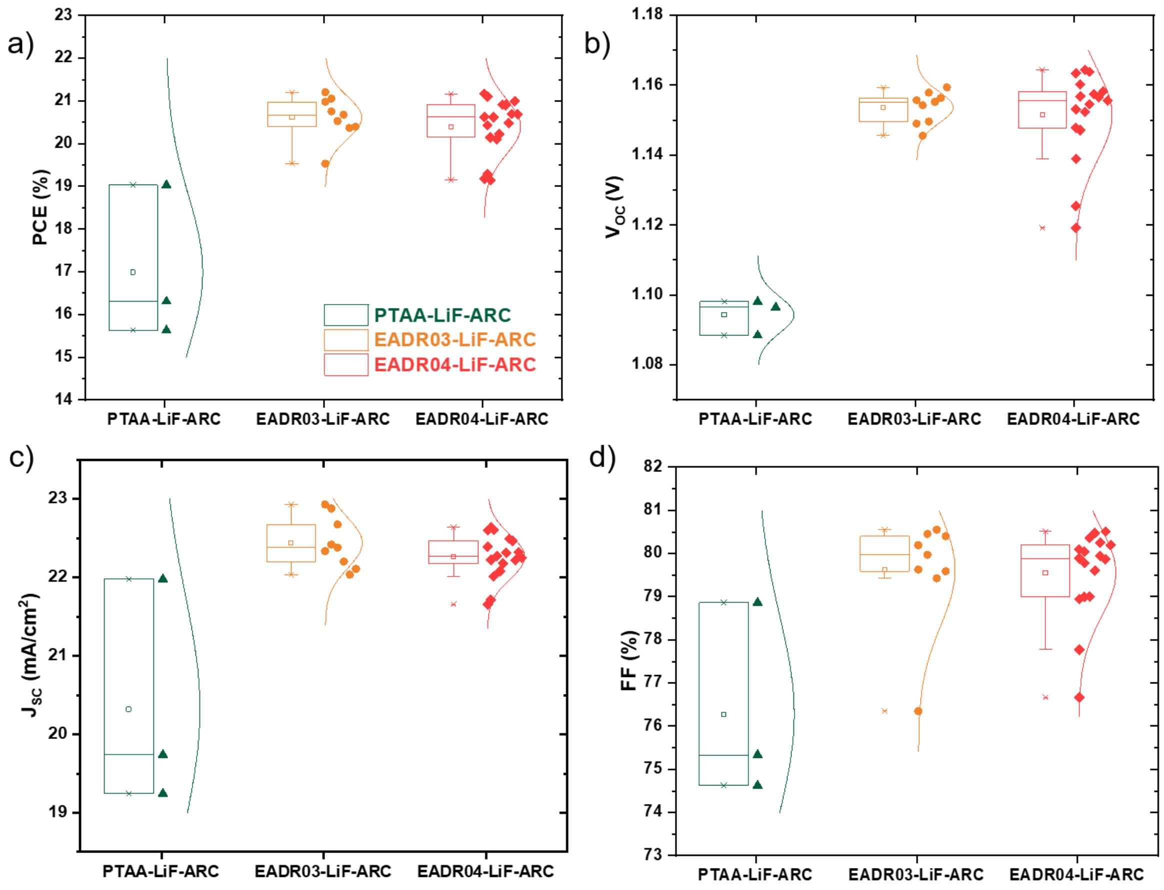

Figure S17. *Device performance statistic total 25 devices from PTAA, EADR03 and EADR04 with LiF and antireflection coating in the devices a) PCE, b) V_{OC}, c) J_{SC}, d) FF.*

J-V measurement under dark condition

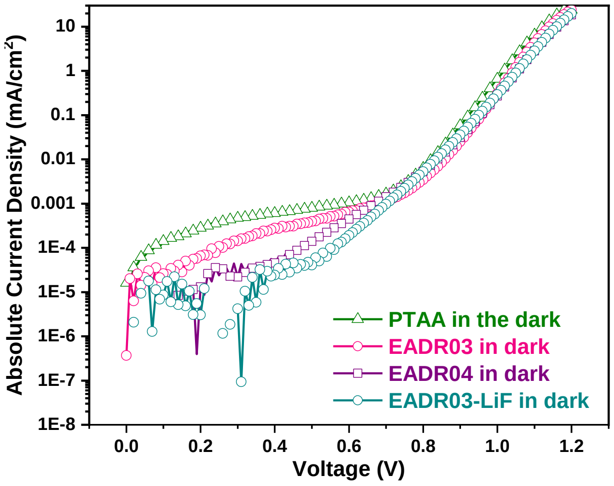

Figure S18. *a) Dark J-V curves of the hole selective contacts.*

Table S7. *Photovoltaic parameters of the best performing devices based on different HSLs with and without UV light exposition with a scan speed of 100 mV/s.*

HSLs	*UV light*	***J_{SC}* (mA/cm^2)**	***V_{OC}* (mV)**	***FF* (%)**	***PCE* (%)**	***HI* (%)**
PTAA	No	21.9	1128	74	18.3	0.02
PTAA	Yes	21.0	1119	76	17.8	0.03
EADR03	No	21.7	1110	79	19.0	0.05
EADR03	Yes	21.9	1100	79	19.0	0.04

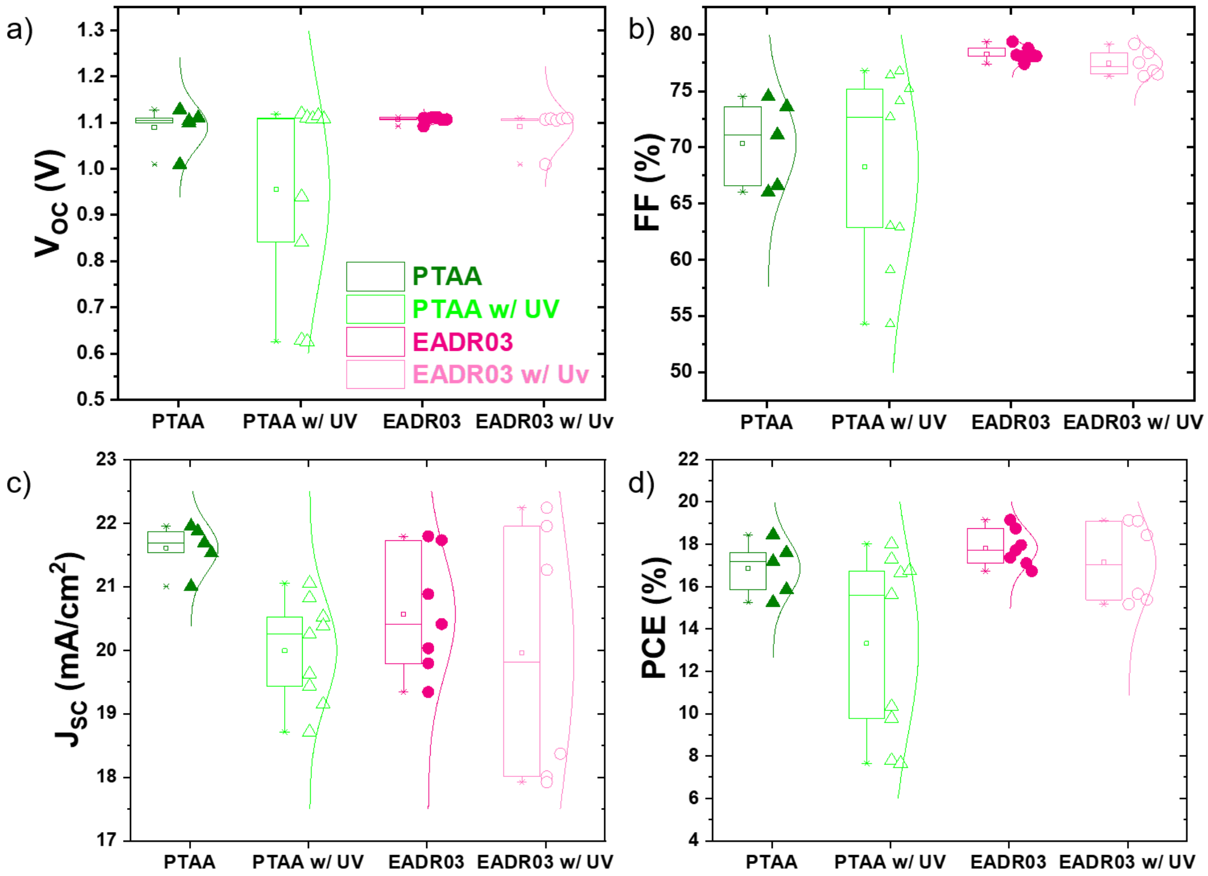

Figure S19. *Device performance statistic total of 25 devices from PTAA and EADR03 with and without UV light exposition.*

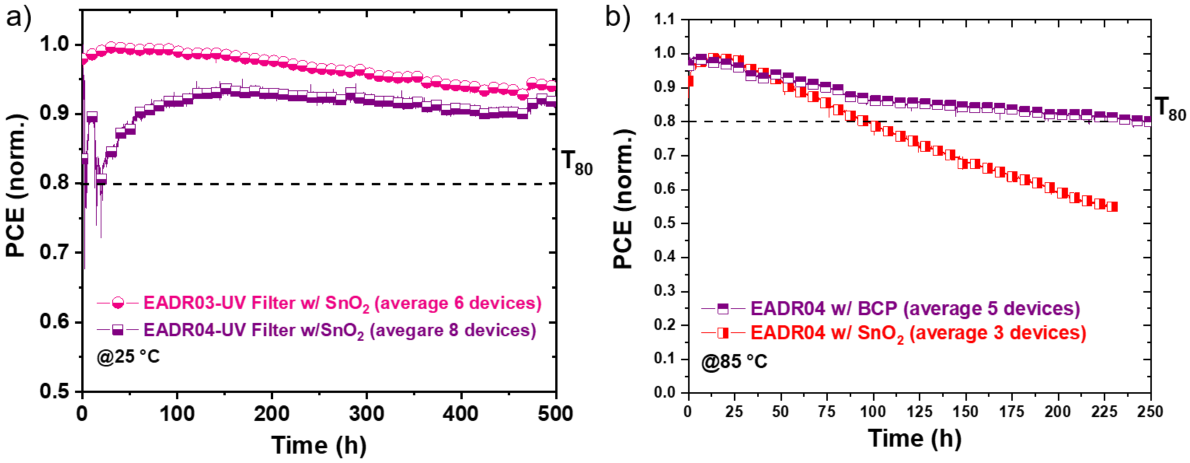

Figure S20. *Long-term continuous maximum power point tracking a) EADR03 and EADR04 based devices with UV Filter and SnO_2 at 25 degree Celsius. b) EADR04 based devices with BCP and SnO_2 at 85 degree Celsius. Note that the values were averaged from different devices from different batches. All the measurements were done in an N_2 atmosphere without encapsulation.*

Table S8. *Estimated T_{80} of the p-i-n perovskite solar cell with EADR03 and EADR04, BCP and SnO_2 from the MPP traces with and without UV filter at different temperatures.*

SAMs	**UV Filter**	**BCP**	**SnO_2**	**Initial PCE (%)**	**Ageing Temperature and Illumination**	**Tracking Time (h)**	**Estimated T_{80} (h)**
EADR03	Yes	No	Yes	18.9	25 °C, metal-halide lamp, 100 mW/cm^2	500	1383
EADR04	Yes	No	Yes	19.4	25 °C, metal-halide lamp, 100 mW/cm^2	500	3582
EADR04	No	Yes	No	20.1	85 °C, metal-halide lamp, 100 mW/cm^2	250	242
EADR04	No	No	Yes	19.9	85 °C, metal-halide lamp, 100 mW/cm^2	225	106

We acknowledge that the at elevated temperature, the metal electrode can interact with perovskite causing degradation such as gold.[10] However, copper has been shown to be stable in using with perovskite, and the degradation using copper is due to presence of moisture and oxygen and the potential oxidation products (*e.g.* $Cu(OH)_2$ or CuO_x).[11] Our study on device stability has been done on inert atmosphere to avoid this particular degradation pathway.

Recent report by Zheng *et al.* showed that BCP can have low thermal stability due to its crystallisation at high temperature (>80 °C).[12] Here, to test whether changing buffer layer to an inorganic material can avoid the further degradation, we used SnO_2 instead of BCP. This enhanced the stability of the device at 25°C, but not at higher temperature as can be seen in Fig. S20. This excludes the degradation pathway due to thermal instability of BCP.

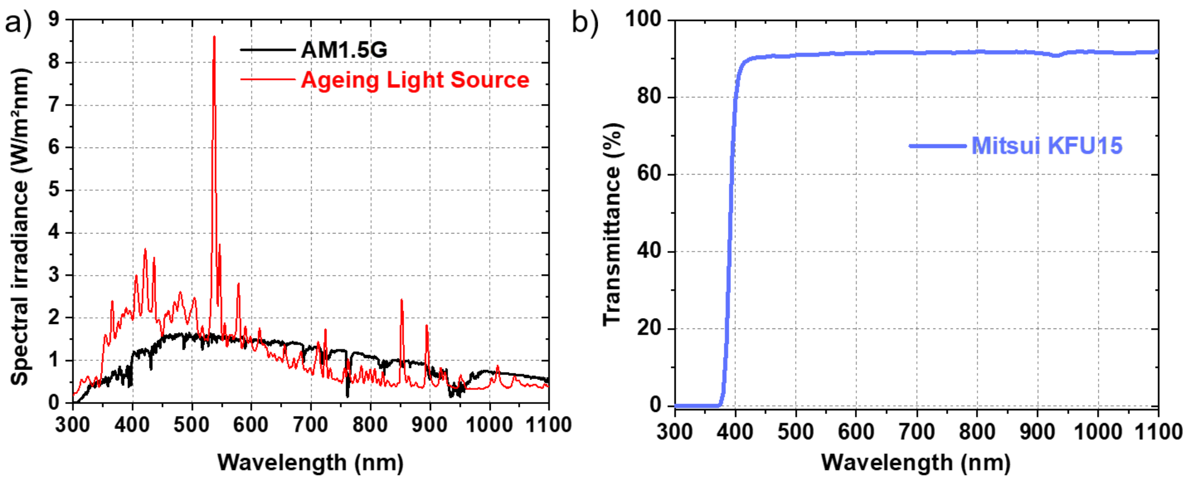

Figure S21. *a) Spectrum distribution of the lamp used for MPP tracking ageing test of perovskite solar cells. b) Transmittance spectra of the UV-blocking foil as named Mitsui KFU15.*

Table S9. *Photovoltaic parameters of different hole selective layers with and without LiF and antireflection coating with a scan speed of 100 mV/s.*

Hole Selective Layers	***LiF***	***ARC***	***Scan Direction***	***Jsc (mA/cm²)***	***Voc (mV)***	***FF (%)***	***PCE (%)***
EADR03	No	No	fwd	22.6	1127	80	20.4
			rev	22.6	1132	80	20.5
EADR03	Yes	No	fwd	21.9	1183	77	19.9
			rev	21.9	1186	79	20.5
EADR03	Yes	Yes	fwd	22.9	1156	80	21.2
			rev	22.9	1155	80	21.1
EADR04	No	No	fwd	22.6	1140	80	20.6
			rev	22.6	1143	79	20.4
EADR04	Yes	No	fwd	22.2	1174	78	20.3
			rev	22.2	1177	80	20.9
EADR04	Yes	Yes	fwd	22.6	1163	80	21.0
			rev	22.6	1164	80	21.0
PTAA	No	No	fwd	21.9	1098	79	18.9
			rev	21.9	1107	77	18.7
PTAA	Yes	No	fwd	21.4	1120	74	17.7
			rev	21.4	1124	78	18.8
PTAA	Yes	Yes	fwd	21.9	1098	79	18.9
			rev	22.0	1105	78	18.9

7. Syntheses of EADR03 and EADR04

7.1. *Synthesis of ethyl 4-(3,6-bis(2,4-dimethoxyphenyl)-9H-carbazol-9-yl)benzoate **(EADR03-COOEt)***

A mixture of ethyl 4-bromobenzoate (0.25 mg, 1.09 mmol), 3,6-bis(2,4-dimethoxyphenyl)-9H-carbazole (0.53 mg, 1.20 mmol), $Pd_2(dba)_3$ (0.10 mg 0.11 mmol), tri-tert-butylphosphine tetrafluoroborate (0.063 mg, 0.22 mmol), sodium tert-butoxide (0.11 mg, 1.2 mmol) are dissolved in 10.0 mL freshly dried toluene in a 25.0 mL two-neck flask under argon atmosphere. The system is purged with argon for 30 minutes. Then, the mixture is refluxed at 115 °C for overnight. The reaction is gradually cooled to room temperature and the solution is concentrated under vacuum. A brine solution (200.0 mL) is added and the solution is extracted with ethyl acetate (EtOAc) (2X100.0 mL). The combined extracts are dried over anhydrous magnesium sulphate, filtered and concentrated under vacuum. The compound is purified by column chromatography (Hexane:EtOAc, 5:1, v:v) and obtained yellow liquid (430 mg, 68% yield). ^{1}H NMR (400 MHz, Chloroform-*d*) δ 8.30 (d, *J* = 8.5 Hz, 2H), 8.23 (dd, *J* = 1.7, 0.7 Hz, 2H), 7.72 (d, *J* = 8.6 Hz, 2H), 7.57 (dd, *J* = 8.5, 1.7 Hz, 2H), 7.49 (dd, *J* = 8.5, 0.7 Hz, 2H), 7.36 (d, *J* = 8.9 Hz, 2H), 6.64 – 6.58 (m, 4H), 4.46 (q, *J* = 7.1 Hz, 2H), 3.88 (s, 6H), 3.82 (s, 6H), 1.45 (t, *J* = 7.1 Hz, 3H). ^{13}C NMR (101 MHz, $CDCl_3$) δ 166.00, 160.05, 157.54, 142.22, 139.44, 131.54, 131.32, 130.87, 128.78, 127.93, 126.15, 124.17, 124.02, 121.27, 109.22, 104.67, 99.11, 61.22, 55.67, 55.48, 14.21.

7.2. *Synthesis of 4-(3,6-bis(2,4-dimethoxyphenyl)-9H-carbazol-9-yl)benzoic acid **(EADR03)***

An aqueous solution of KOH (382 mg, 6.80 mmol) is added to 4-(3,6-bis(2,4-dimethoxyphenyl)-9*H*-carbazol-9-yl)benzoate (400 mg, 0.68 mmol). Then, to this aqueous phase, a methanol and tetrahydrofuran (1:1) mixture is added to maintain complete dissolution at 85 °C. The mixture is refluxed at 85 °C for overnight. The reaction is gradually cooled to room temperature and the solution is concentrated under vacuum. 200.0 mL of water is added and the resulting aqua layer is treated with 2M HCl to obtain an off-white color, which is filtered and dried under vacuum, to afford 4-(3,6-bis(2,4-dimethoxyphenyl)-9H-carbazol-9-yl)benzoic acid (340 mg, 89% yield). ESI-MS m/z calc. for $C_{35}H_{28}NO_6^-$ (M-): 558.1922; found: 558.1912. Elemental Anal. calcd. for $C_{35}H_{29}NO_6$: C, 75.12; H, 5.22; N, 2.50. Found: C, 70.21; H, 4.90; N, 2.21. ^{1}H NMR (400 MHz, DMSO-*d*$_6$) δ 8.28 (d, *J* = 1.7 Hz, 2H), 8.25 (d, *J* = 8.6 Hz, 2H), 7.84 (d, *J* = 8.5 Hz, 2H), 7.54 (dd, *J* = 8.6, 1.6 Hz, 2H), 7.50 (d, *J* = 8.5 Hz, 2H), 7.33 (d, *J* = 8.3 Hz, 2H), 6.70 (d, *J* = 2.4 Hz, 2H), 6.66 (dd, *J* = 8.4, 2.4 Hz, 2H), 3.83 (s, 6H), 3.79 (s, 6H). ^{13}C NMR (101 MHz, DMSO) δ 167.24, 160.26, 157.64, 141.52, 139.08, 131.79, 131.69, 131.25, 129.70, 128.51, 126.55, 123.67, 123.49, 121.42, 109.70, 105.77, 99.43, 56.05, 55.75.

*7.3. Synthesis of methyl 4'-(3,6-bis(2,4-dimethoxyphenyl)-9H-carbazol-9-yl)-[1,1'-biphenyl]-4-carboxylate **(EADR04-COOMe)***

A mixture of methyl 4'-bromo-[1,1'-biphenyl]-4-carboxylate (0.25 mg, 0.85 mmol), 3,6-bis(2,4-dimethoxyphenyl)-9H-carbazole (0.45 mg, 1.03 mmol), $Pd_2(dba)_3$ (0.16 mg 0.17 mmol), tri-tert-butylphosphine tetrafluoroborate (0.10 mg, 0.34 mmol), sodium tert-butoxide (0.09 mg, 0.94 mmol) are dissolved in 15.0 mL freshly dried toluene in a 50.0 mL two-neck flask under argon atmosphere. The system is purged with argon for 30 minutes. Then, the mixture is refluxed at 115 °C for overnight. The reaction is gradually cooled to room temperature and the solution is concentrated under vacuum. A brine solution (200.0 mL) is added and the solution is extracted with ethyl acetate (EtOAc) (2X100.0 mL). The combined extracts are dried over anhydrous magnesium sulphate, filtered and concentrated under vacuum. The compound is purified by column chromatography (Hexane:EtOAc, 2:1, v:v) and recrystallized is performed in EtOH to give light yellow color crystals (300 mg, 53%). ^{1}H NMR (400 MHz, Chloroform-d) δ 8.26 (dd, J = 1.7, 0.7 Hz, 2H), 8.20 – 8.17 (m, 2H), 7.87 (d, J = 8.5 Hz, 2H), 7.80 – 7.76 (m, 2H), 7.73 (d, J = 8.5 Hz, 2H), 7.58 (dd, J = 8.5, 1.7 Hz, 2H), 7.50 (dd, J = 8.5, 0.7 Hz, 2H), 7.38 (d, J = 9.0 Hz, 2H), 6.65 – 6.60 (m, 4H), 3.98 (s, 3H), 3.88 (s, 6H), 3.83 (s, 6H). ^{13}C NMR (101 MHz, CDCl3) δ 166.96, 160.01, 157.56, 144.71, 139.92, 138.74, 138.04, 131.57, 130.47, 130.30, 129.21, 128.69, 127.82, 127.24, 127.04, 124.35, 123.76, 121.24, 109.24, 104.69, 99.14, 55.68, 55.66, 55.48, 55.46, 52.20.

2nd

*7.4. Synthesis of 4'-(3,6-bis(2,4-dimethoxyphenyl)-9H-carbazol-9-yl)-[1,1'-biphenyl]-4-carboxylic acid **(EADR04)***

An aqueous solution of KOH (0.30 mg, 4.60 mmol) is added to methyl 4'-(3,6-bis(2,4-dimethoxyphenyl)-9H-carbazol-9-yl)-[1,1'-biphenyl]-4-carboxylate **(EADR04-COOMe)** (0.30 mg, 0.46 mmol). Then, to this aqueous phase, a methanol and tetrahydrofuran (1:1) mixture is added to maintain complete dissolution at 85 °C. The mixture is refluxed at 85 °C for overnight. The reaction is gradually cooled to room temperature and the solution is concentrated under vacuum. 200.0 mL of water is added, and the resulting aqua layer is acidified with 2M HCl. Then, the crude product is purified with flash chromatography (140 mg, 48% yield). ESI-MS m/z calc. for $C_{41}H_{32}NO_6^-$ (M-):634.2235; found: 634.2246. Elemental Anal. calcd. for $C_{41}H_{33}NO_6$: C, 77.46; H, 5.23; N, 2.20. Found: C, 74.22; H, 5.38; N, 2.23. ^{1}H NMR (400 MHz, DMSO-*d*6) δ 13.04 (s, 1H), 8.29 (d, J = 1.7 Hz, 2H), 8.09 (dd, J = 10.8, 8.5 Hz, 4H), 7.96 (d, J = 8.4 Hz, 2H), 7.82 (d, J = 8.6 Hz, 2H), 7.54 (dd, J = 8.6, 1.7 Hz, 2H), 7.51 – 7.46 (m, 2H), 7.38 – 7.29 (m, 2H), 6.74 – 6.64 (m, 4H), 3.83 (s, 6H), 3.80 (s, 6H). ^{13}C NMR (101 MHz, DMSO) δ 167.57, 160.23, 157.66, 143.86, 139.52, 138.36, 137.63, 137.61, 131.69, 130.91, 130.57, 129.17, 128.42, 127.45, 127.38, 123.64, 123.45, 121.43, 109.61, 105.76, 99.47, 56.07, 56.02, 55.76, 55.72, 40.64, 40.43, 40.22, 40.01, 39.80, 39.59, 39.38.

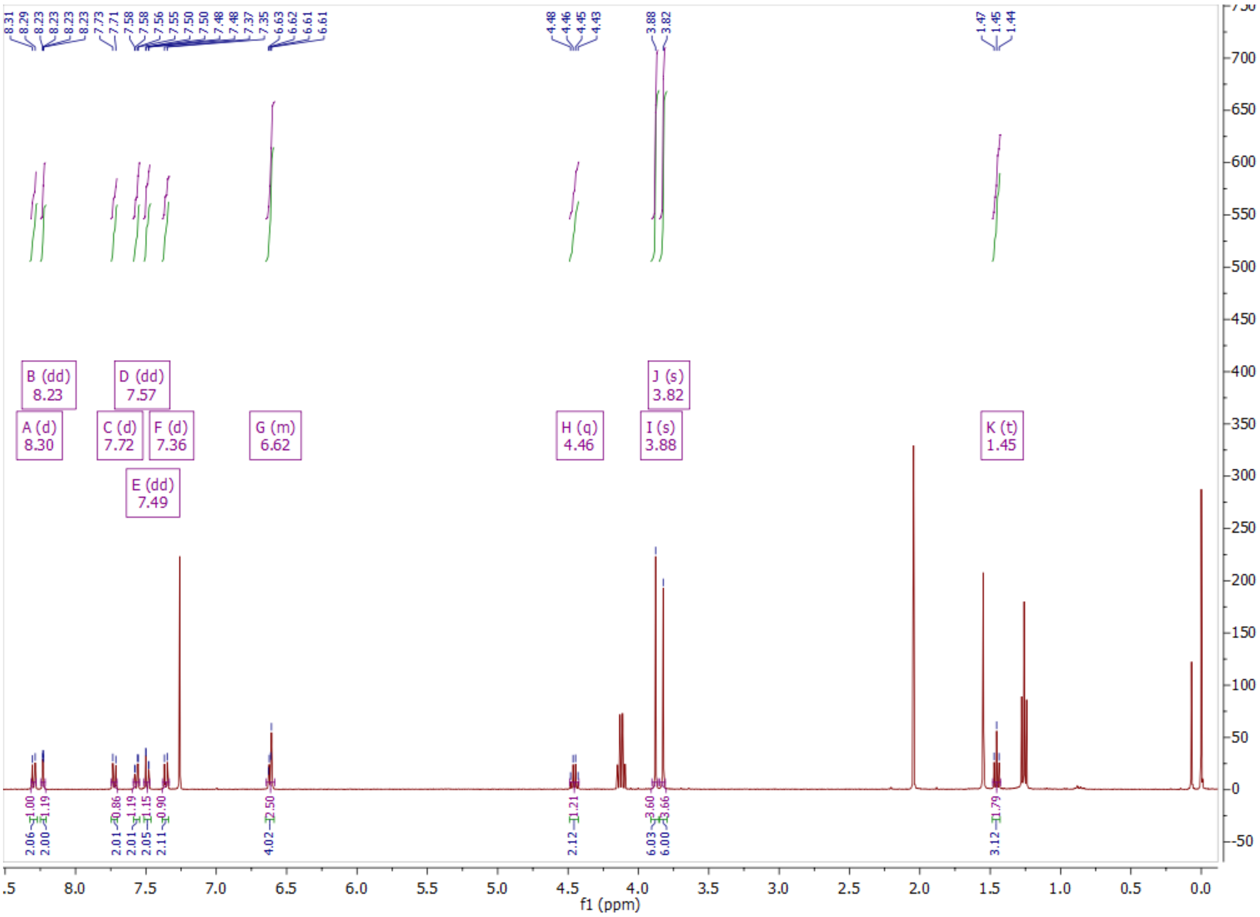

Figure S22. *^{1}H NMR spectrum of EADR03-COOEt*

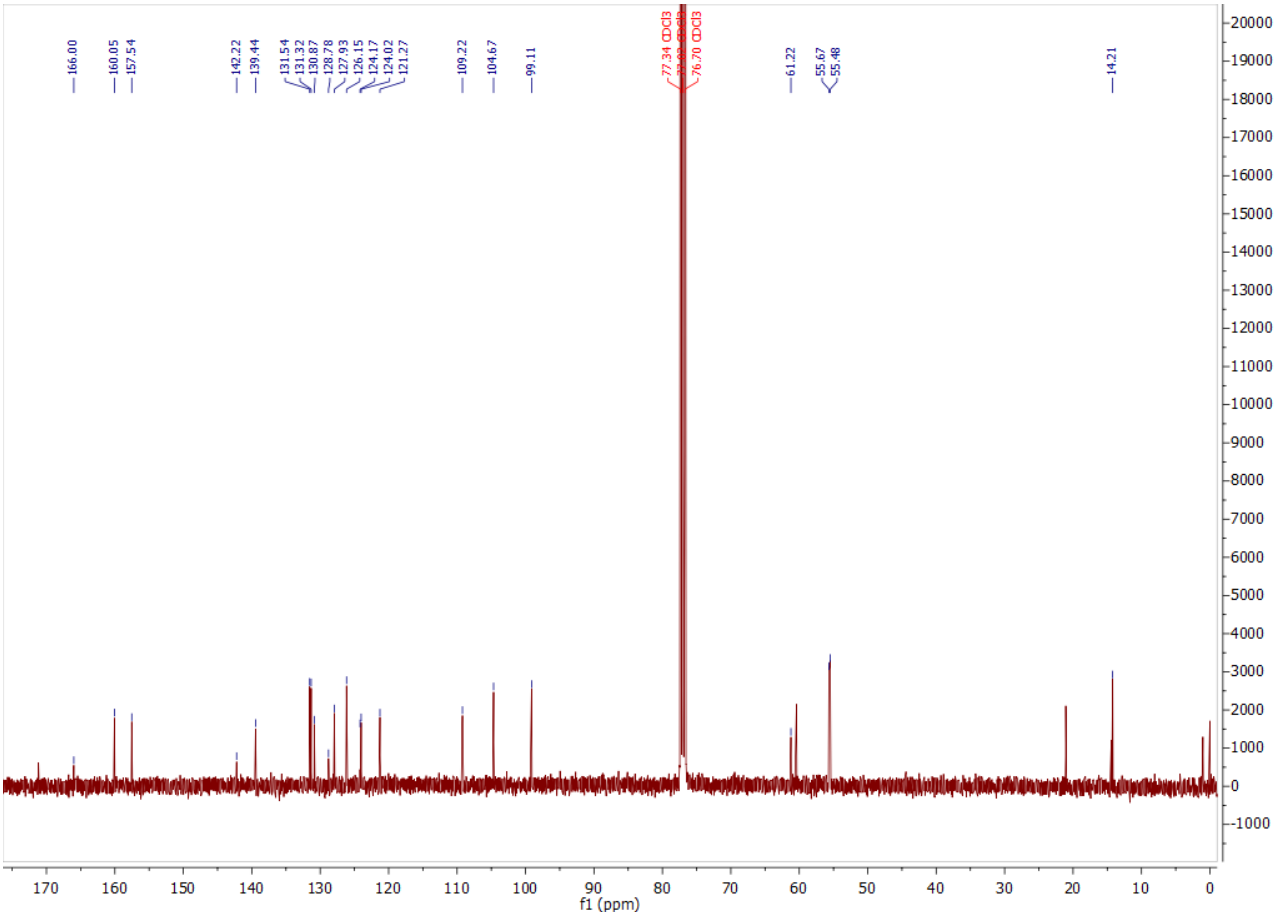

Figure S23. *^{13}C NMR spectrum of EADR03-COOEt*

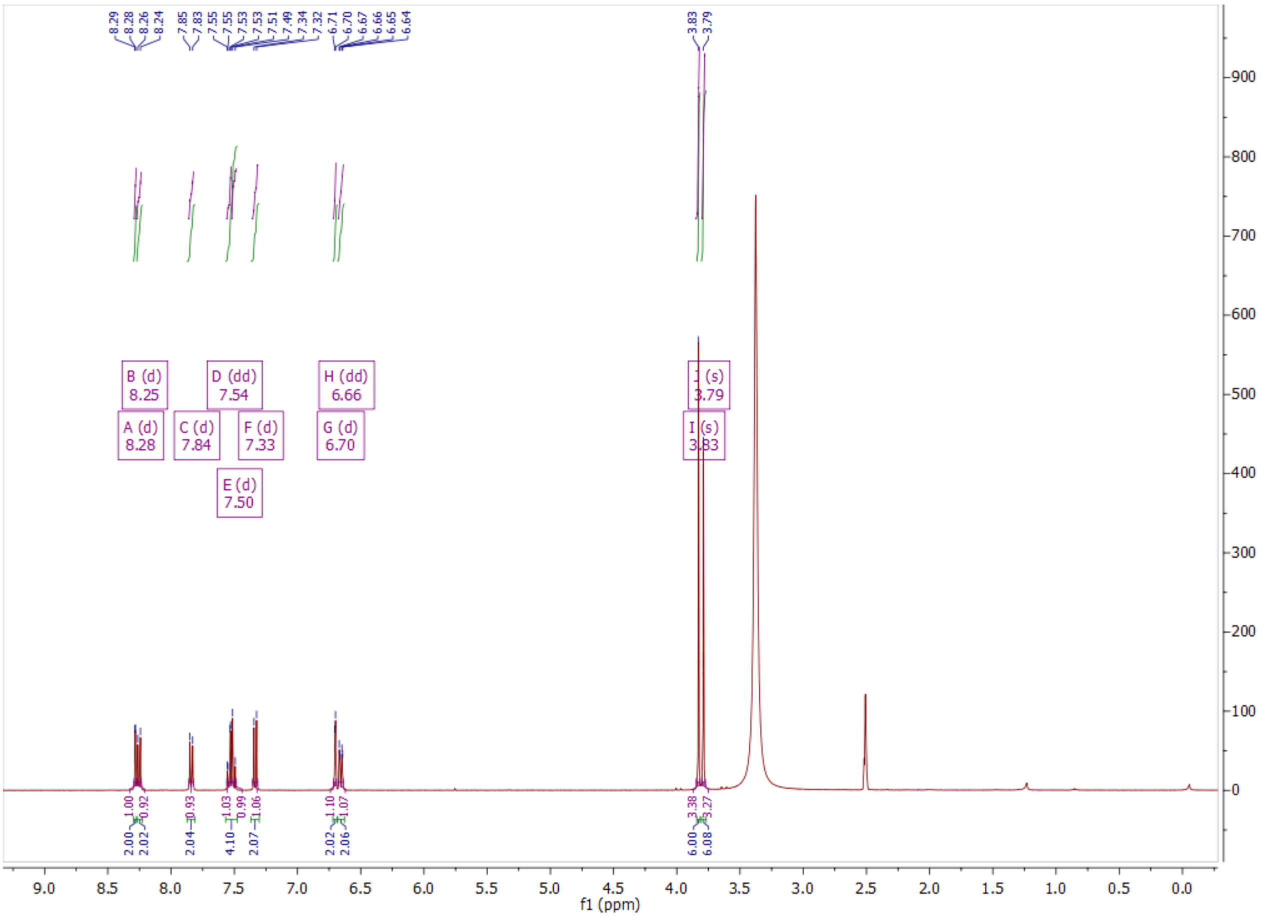

Figure S24. *^{1}H NMR spectrum of EADR03*

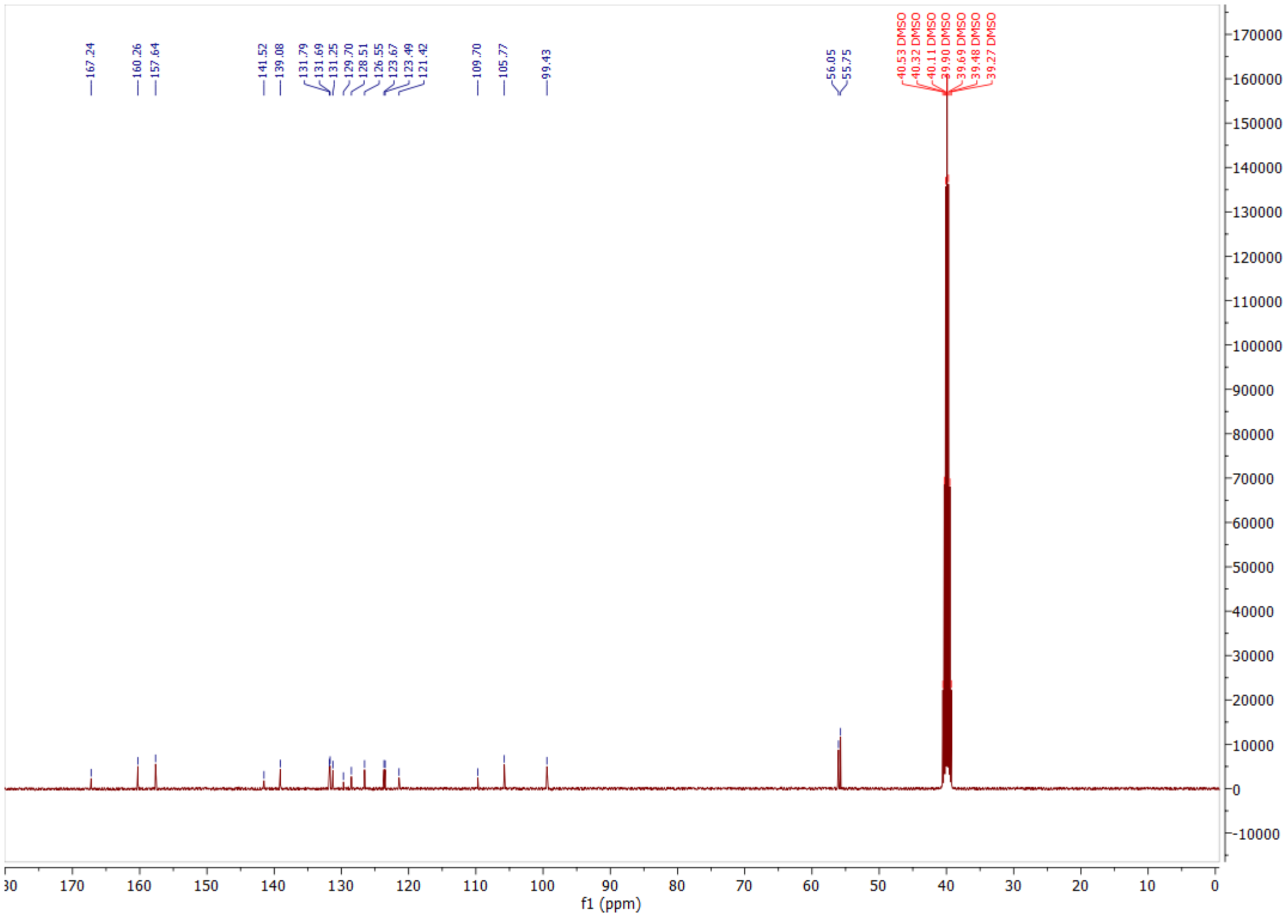

Figure S25. *^{13}C NMR spectrum of EADR03*

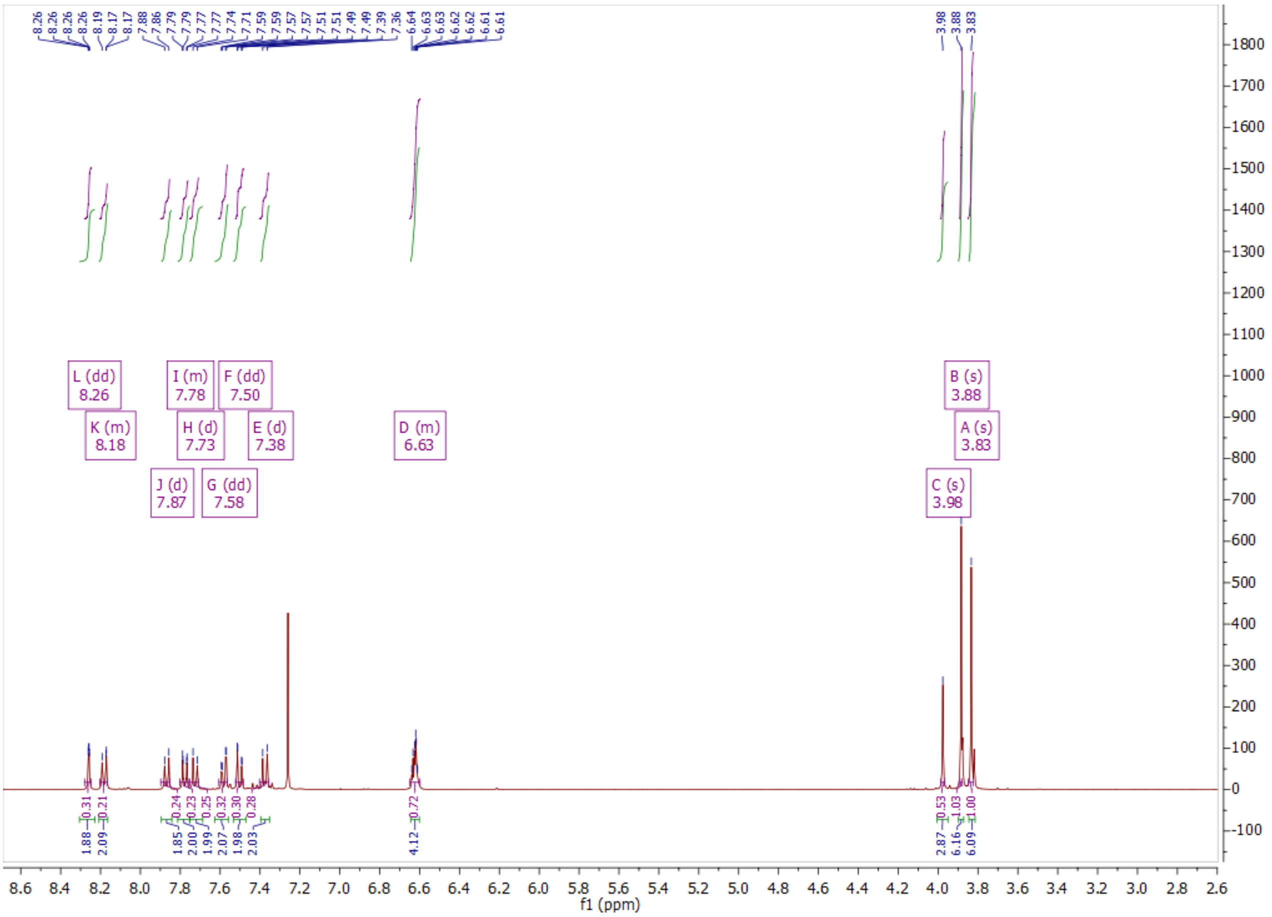

Figure S26. *^{1}H NMR spectrum of EADR04-COOMe*

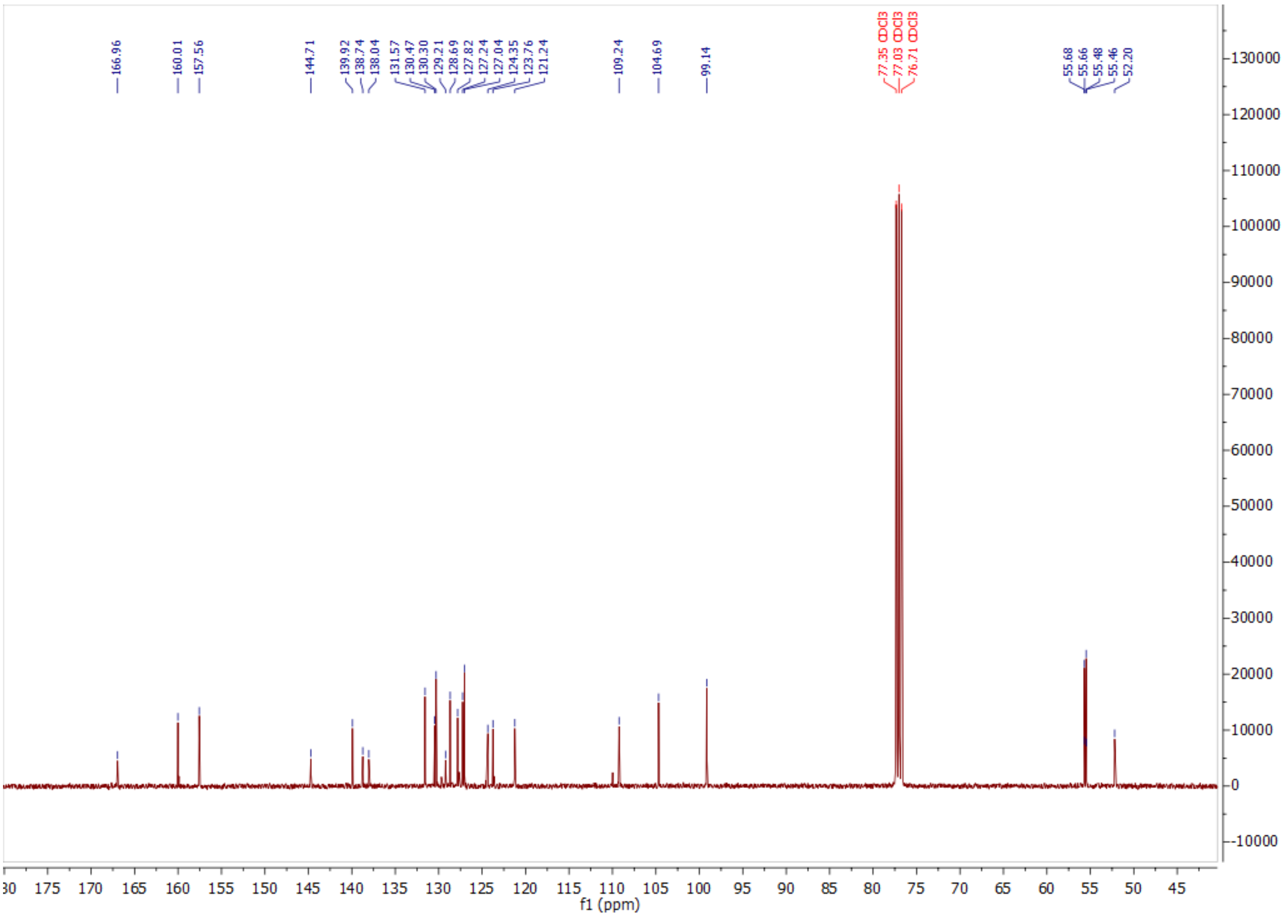

Figure S27. *^{13}C NMR spectrum of EADR04-COOMe*

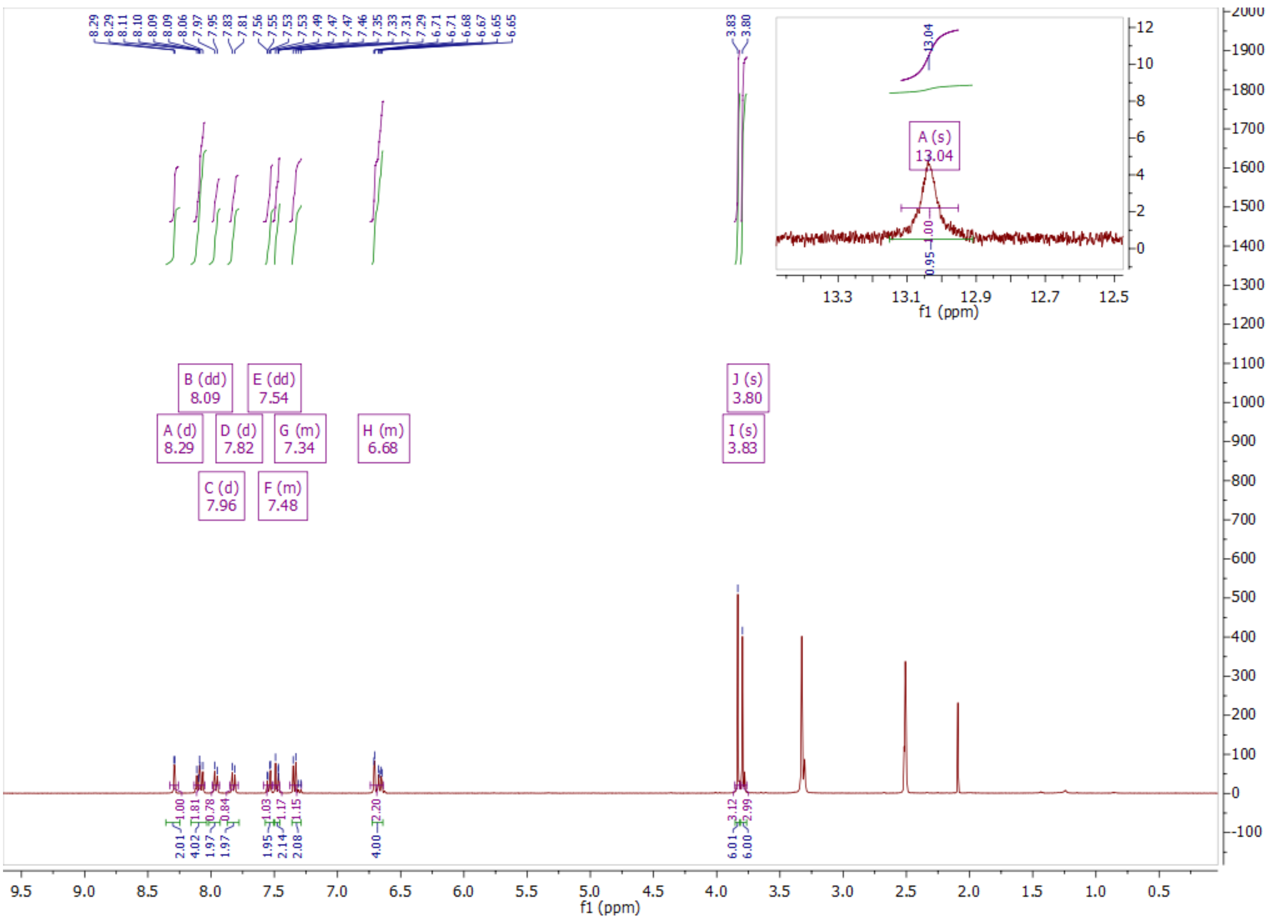

Figure S28. *^{1}H NMR spectrum of EADR04*

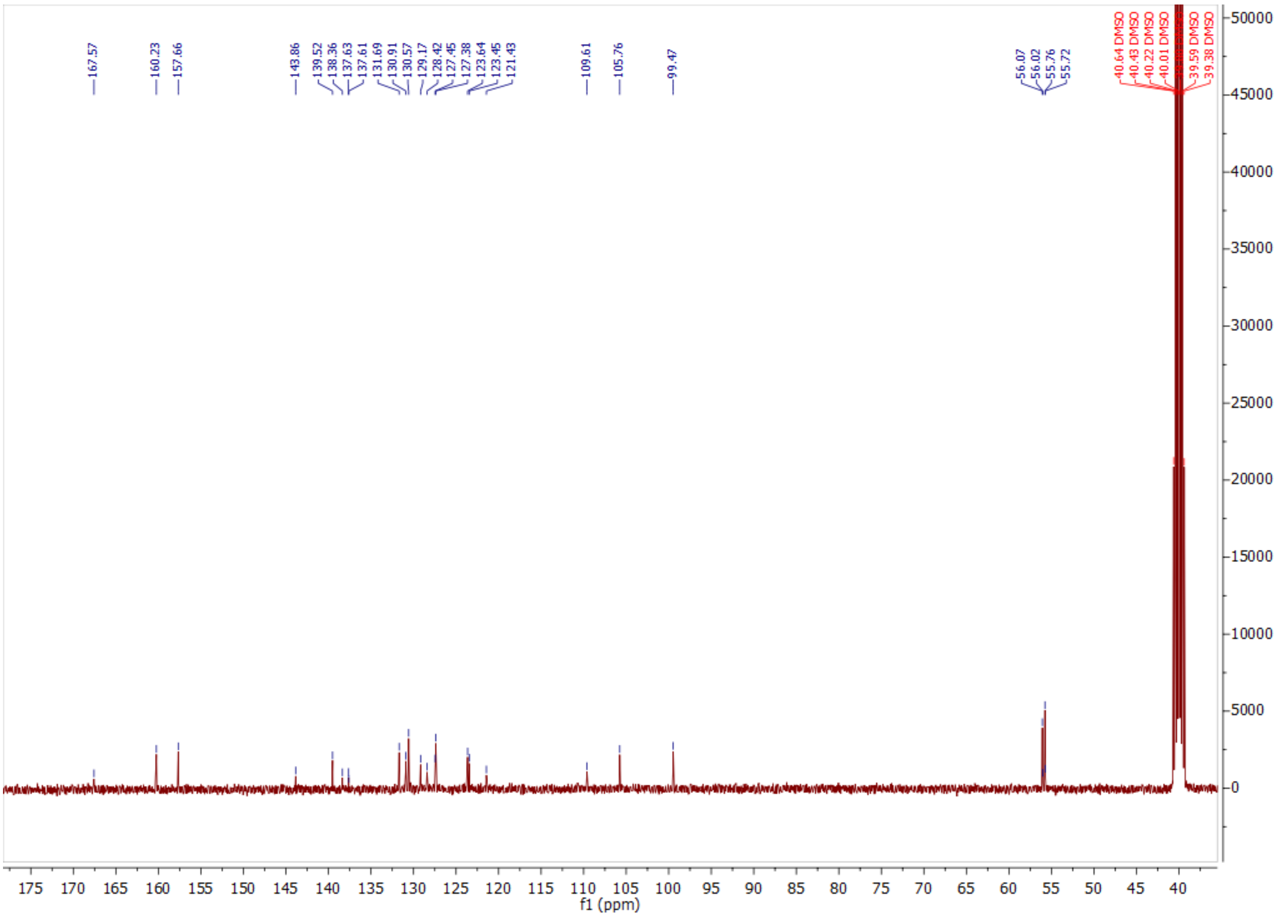

Figure S29. *^{13}C NMR spectrum of EADR04*

Analysis Name	W:\Data\191018\191018_EADR03_RA2_01_25091.d			
Method	tune_low_negative-hplc-exactas2min.m	Operator	ICIQ	
Sample Name	191018_EADR03	Instrument / Ser#	micrOTOF	213750.1
Comment	0.1ppm, MeOH injection			394

Acquisition Parameter

Source Type	ESI	Ion Polarity	Negative	Set Nebulizer	1.2 Bar
Focus	Active			Set Dry Heater	180 °C
Scan Begin	50 m/z	Set Capillary	4000 V	Set Dry Gas	8.0 l/min
Scan End	3000 m/z	Set End Plate Offset	-500 V	Set Divert Valve	Source

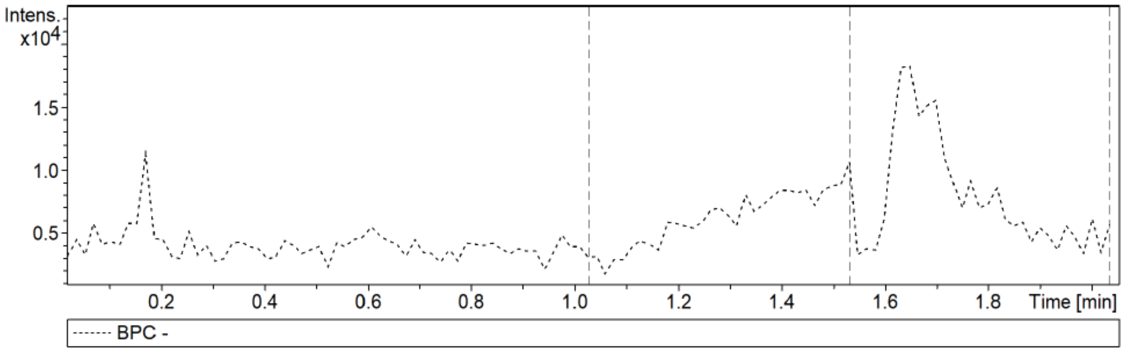

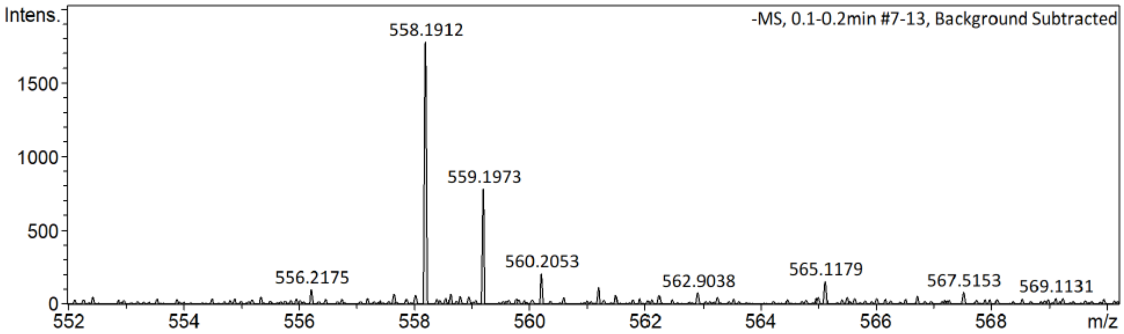

Meas. m/z	Ion Formula	m/z	|err| [ppm]	err [mDa]	mSigma	e$^-$ Conf	z
558.1912	C35H28NO6	558.1922	1.9	1.1	39.1	even	1-

Figure S30. *ESI-MS of EADR03*

Analysis Name	W:\Data\191018\191018_EADR04_RA3_01_25089.d			
Method	tune_low_negative-hplc-exactas2min.m	Operator	ICIQ	
Sample Name	191018_EADR04	Instrument / Ser#	micrOTOF	213750. 394
Comment	0.1ppm, MeOH injection			

Acquisition Parameter

Source Type	ESI	Ion Polarity	Negative	Set Nebulizer	1.2 Bar
Focus	Active			Set Dry Heater	180 °C
Scan Begin	50 m/z	Set Capillary	4000 V	Set Dry Gas	8.0 l/min
Scan End	3000 m/z	Set End Plate Offset	-500 V	Set Divert Valve	Source

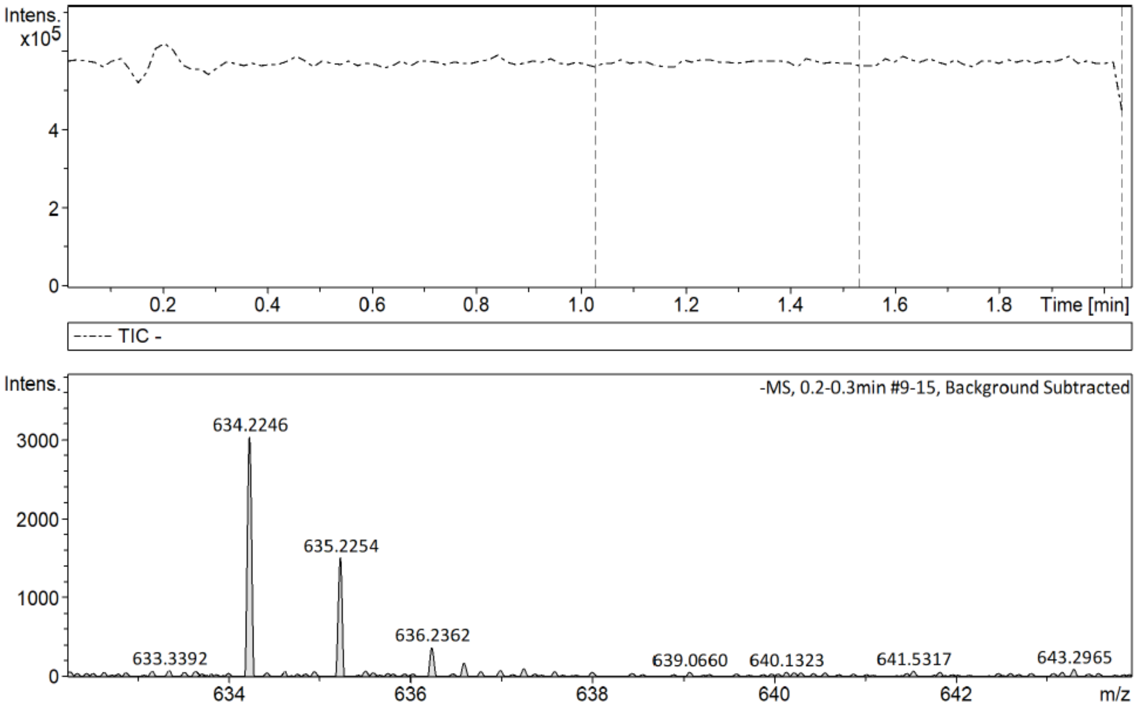

Meas. m/z	Ion Formula	m/z	|err| [ppm]	err [mDa]	mSigma	e^- Conf	z
634.2246	C41H32NO6	634.2235	1.7	-1.1	23.5	even	1-

Figure S31. *ESI-MS of EADR04*

8. References

1. Rodríguez-Seco, C. *et al.* Minimization of Carrier Losses for Efficient Perovskite Solar Cells through Structural Modification of Triphenylamine Derivatives. *Angew. Chemie* **132**, 5341–5345 (2020).
2. Wang, B., Zeng, Q., Sun, Z., Xue, S. & Liang, M. Molecularly engineering of truxene-based dopant-free hole-transporting materials for efficient inverted planar perovskite solar cells. *Dye. Pigment.* **165**, 81–89 (2019).
3. Saliba, M. *et al.* How to Make over 20% Efficient Perovskite Solar Cells in Regular (n–i–p) and Inverted (p–i–n) Architectures. *Chem. Mater.* **30**, 4193–4201 (2018).
4. Lauermann, I. & Steigert, A. CISSY: A station for preparation and surface/interface analysis of thin film materials and devices. *J. large-scale Res. Facil. JLSRF* **2**, A67 (2016).
5. Shippony, Z. & Read, W. G. A highly accurate Voigt function algorithm. *J. Quant. Spectrosc. Radiat. Transf.* **50**, 635–646 (1993).
6. Wang, Q. *et al.* Managing Phase Purities and Crystal Orientation for High-Performance and Photostable Cesium Lead Halide Perovskite Solar Cells. *Sol. RRL* **4**, 2000213 (2020).
7. Rakocevic, L. *et al.* Reliable Performance Comparison of Perovskite Solar Cells Using Optimized Maximum Power Point Tracking. *Sol. RRL* **3**, 1800287 (2019).
8. Saliba, M. *et al.* Cesium-containing triple cation perovskite solar cells: Improved stability, reproducibility and high efficiency. *Energy Environ. Sci.* **9**, 1989–1997 (2016).
9. Saidaminov, M. I. *et al.* Suppression of atomic vacancies via incorporation of isovalent small ions to increase the stability of halide perovskite solar cells in ambient air. *Nat. Energy* **3**, 648–654 (2018).
10. Domanski, K. *et al.* Not All That Glitters Is Gold: Metal-Migration-Induced Degradation in Perovskite Solar Cells. *ACS Nano* **10**, 6306–6314 (2016).
11. Zhao, J. *et al.* Is Cu a stable electrode material in hybrid perovskite solar cells for a 30-year lifetime? *Energy Environ. Sci.* **9**, 3650–3656 (2016).
12. Zheng, X. *et al.* Enhanced thermal stability of inverted perovskite solar cells by interface modification and additive strategy. *RSC Adv.* **10**, 18400–18406 (2020).